Published in final edited form as:

Structure. 2021 September 02; 29(9): 975–988.e5. doi:10.1016/j.str.2021.04.011.

Bi-partite binding of the N-terminus of Skp2 to cyclin A

Susan Kelso[1,2], **Stephen Orlicky**[1], **Jonah Beenstock**[1], **Derek F. Ceccarelli**[1], **Igor Kurinov**[3], **Gerald Gish**[1], **Frank Sicheri**[1,2,4,5,*]

[1] Lunenfeld-Tanenbaum Research Institute, Sinai Health System, Toronto, Ontario M5G 1X5, Canada

[2] Department of Molecular Genetics, University of Toronto, Ontario M5S 1A8, Canada

[3] Department of Chemistry and Chemical Biology, Cornell University, NE-CAT, Argonne, Illinois 60439, USA

[4] Department of Biochemistry, University of Toronto, Ontario M5S 1A8, Canada

[5] Lead contact

Summary

Skp2 and cyclin A are cell cycle regulators that control the activity of CDK2. Cyclin A acts as an activator and substrate recruitment factor of CDK2, while Skp2 mediates the ubiquitination and subsequent destruction of the CDK inhibitor protein p27. The N-terminus of Skp2 can interact directly with cyclin A but is not required for p27 ubiquitination. To gain insight into this poorly understood interaction, we have solved the 3.2 Å X-ray crystal structure of the N-terminus of Skp2 bound to cyclin A. The structure reveals a bi-partite mode of interaction with two motifs in Skp2 recognizing two discrete surfaces on cyclin A. The uncovered binding mechanism allows for a rationalization of the inhibitory effect of Skp2 on CDK2-cyclin A kinase activity towards RxL motif containing substrates and raises the possibility that other intermolecular regulators and substrates may use similar non-canonical modes of interaction for cyclin targeting.

Graphical Abstract

*Correspondence: sicheri@lunenfeld.ca.

Author Contributions

Conceptualization, S.K., S.O., and F.S.; Investigation, S.K., S.O., J.B., D.C., I.K., and G.G.; Writing and visualization, S.K. and F.S.; Funding acquisition and supervision, F.S.

Declaration of Interests

F.S. is a founder and consultant of Repare Therapeutics.

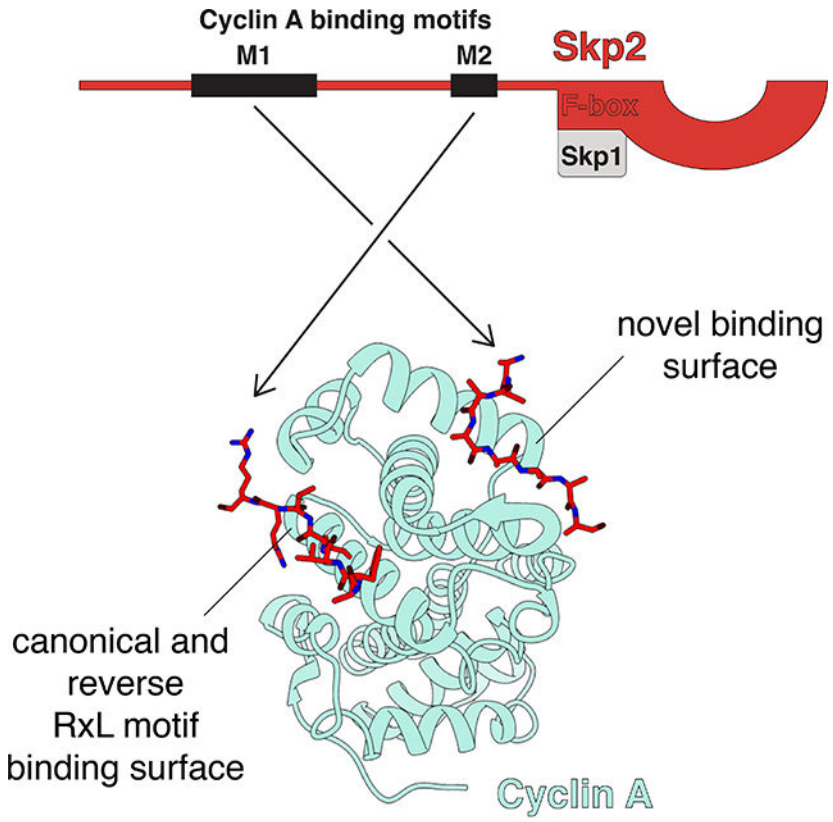

eTOC Blurb:

Kelso et al. demonstrate that the Skp2 N-terminus contains two motifs that bind cyclin A but not cyclin E. One resembles the known RxL cyclin binding motif, but in the reverse direction. Binding of the Skp2 N-terminus to cyclin A blocks recruitment of CDK substrates.

Introduction

Progression through the cell cycle in eukaryotes is regulated by the sequential activation and repression of cyclin-dependent kinases (CDKs). The spatial and temporal regulation of CDK activity is dependent on the presence of critical intermolecular binding partners, namely cyclin activators and CDK inhibitors, as well as by phosphorylation events within the CDK kinase domain (summarized in Hochegger et al., 2008). The abundance of cyclins and CDK inhibitors is cell cycle regulated, and their degradation is commonly controlled by ubiquitin-directed proteolysis.

Ubiquitination is catalyzed by a cascade of E1/E2/E3 enzymes, which begins with activation of ubiquitin (Ub) in an ATP dependent manner and terminates with the covalent attachment of Ub to lysine residues in the target proteins. Iterative rounds of this process can build poly Ub chains on a target by virtue that the seven lysine residues (K6, K11, K27, K29, K33, K48, K63) and the free amino-terminus (M1) of Ub can serve as modification sites for ubiquitination. Canonically, Ub chains built by K48 linkages direct target proteins

to the 26S proteasome for unfolding and cleavage into small peptides, thereby ensuring irreversible functional inactivation (reviewed in Komander and Rape, 2012). Of the E1/E2/E3 ubiquitination machinery, the E3 enzyme imparts selectivity to the modification process by direct binding to substrates. While the human genome encodes greater that 600 E3s, only a small subset have been studied in great detail. The SCF (**S**kp1-**C**ul1-**F**-box) ligases represent a family of 69 multi-subunit E3s that were initially discovered based on the roles of select members in cell cycle regulation (Feldman et al., 1997; Skowyra et al., 1997). SCF ligases contain the 3 core subunits Skp1, Cul1, and Rbx1, together with a variable subunit called the F-box protein that mediates selective binding of substrates. F-box proteins share a common element termed the F-box domain that binds Skp1, allowing for integration of the F-box protein into the larger SCF ligase complex (Chang et al., 1996).

Skp2 is a founding member of the F-box protein family and best known for its role in activating the cyclin-dependent kinase CDK2 at the G1- to S-phase transition of the cell cycle. As cyclin levels rise in late G1-phase, CDK2-cyclin A/E complexes are maintained in an inactive state by binding to the CDK inhibitor protein $p27^{Kip1}$ (hereafter referred to as p27). p27 binds across both CDK2 and cyclins, the latter by use of a linear motif (RNLFG) that engages the 'hydrophobic patch' on the cyclin (Russo et al., 1996). In the nucleus, p27 is ubiquitinated by SCF^{Skp2} (superscript denotes the F-box protein of the SCF complex) in response to phosphorylation of p27 on T187 (Carrano et al., 1999; Sutterlüty et al., 1999; Tsvetkov et al., 1999). Skp2 recruits phosphorylated p27 (as part of inhibited p27-CDK2-cyclin complexes) to its respective ligase SCF^{Skp2} by recognition of both CDK2 and the phosphorylated motif (pT187) within the C-terminus of p27 (Montagnoli et al., 1999). Recognition of both CDK2 and the C-terminus of p27 requires the bridging adaptor protein Cks1, which binds to the C-terminal leucine-rich repeat (LRR) domain of Skp2 (Ganoth et al., 2001; Spruck et al., 2001) (Figure 1A). This mode of recognition is used for CDK2-cyclin A or CDK2-cyclin E complexes, which are both present at the end of G1-phase (Montagnoli et al., 1999). Crystal structures of Skp2, Cks1, CDK2, cyclin A, and p27 in a variety of subcomplexes have uncovered the basis for their interaction in atomic detail (Bourne et al., 1996; Jeffrey et al., 1995; Russo et al., 1996; Schulman et al., 2000). Formation of the ternary complex involving SCF^{Skp2}, Cks1, CDK2-cyclin A/E and phosphorylated p27 triggers the ubiquitination and degradation of p27, rendering CDK2-cyclin A/E active to phosphorylate downstream substrates that promote cell cycle entry into S-phase.

N-terminal to the F-box domain, Skp2 harbours a 94-amino acid disordered region that mediates multiple functions (Figure S1). First, Skp2 residues 65 to 78 comprises a nuclear localization signal motif required for nuclear transport (Gao et al., 2009). Second, Skp2 residues 3 to 6 (comprising a destruction- or D-box motif) and residues 46 to 94, allow binding to Cdh1, the substrate adaptor of the E3 ligase, APC^{Cdh1} (Anaphase-promoting complex; superscript denotes the substrate adaptor). This allows APC^{Cdh1} to regulate Skp2 protein levels during G1 phase of the cell cycle (Bashir et al., 2004; Wei et al., 2004). Recognition of Skp2 by APC^{Cdh1} in turn is regulated by modifications of residues within the N-terminus including phosphorylation at S72 and S75 and acetylation at K68 and K71 (Gao et al., 2009; Inuzuka et al., 2012). Finally, the N-terminus makes interactions with other

proteins for which no clear biological function has been ascribed, including Rb (Ji et al., 2004) and cyclin A.

Prior to uncovering a role for Skp2 in p27 ubiquitination, Skp1 and Skp2 were identified as binding partners of CDK2-cyclin A complexes (Zhang et al., 1995). Later studies revealed that both the N-terminus of Skp2 and C-terminus of Skp2 were sufficient for binding to CDK2-cyclin A (Yam et al., 1999). Deletion analysis localized a motif within the N-terminus of Skp2 (residues 28 to 48) that engages in direct contacts specifically with cyclin A (Ji et al., 2006) and not with other CDK-cyclin complexes such as CDK2-cyclin E and CDK4-cyclin D1 (Ji et al., 2006). Interestingly, two CDK inhibitors and substrates of SCF^{Skp2}, p21 and p27, were shown to compete with the N-terminus of Skp2 for binding to CDK2-cyclin A (Ji et al., 2006). The functional consequence of this behaviour is not understood.

Recently, Salamina et al. (2021) employed Hydrogen-Deuterium Exchange Mass Spectrometry (HDX-MS) to localize an elongated interaction surface on cyclin A for the N-terminus of Skp2. This surface comprised the well-characterized ‘hydrophobic patch’ that binds RxL (either (K/R)xLΦ or (K/R)xLxΦ, where x is any residue and Φ is a large hydrophobic residue) consensus motifs in CDK-cyclin substrates and regulators (Adams et al., 1996; Chen et al., 1996; Schulman et al., 1998) and a contact region not previously implicated in protein-protein interactions (Salamina et al., 2021). Issues that remain to be addressed include which specific regions in the Skp2 N-terminus mediate complementary binding to the identified surfaces on cyclin A. The finding that the N-terminus of Skp2 binds the hydrophobic patch of cyclin A is particularly surprising since the N-terminus of Skp2 lacks an apparent RxL motif.

To better understand the molecular details of specific binding between the N-terminus of Skp2 and cyclin A, we embarked on studies to visualize the atomic structure of this interaction using X-ray crystallography. The resultant structure revealed that Skp2 binds cyclin A via two linear motifs, including a non-canonical RxL motif that binds to the hydrophobic patch of cyclin A in a reverse orientation. Binding of Skp2 to cyclin A can disrupt the phosphorylation of RxL-containing substrates of CDK2 without completely inhibiting kinase activity.

Results

Two motifs within the N-terminus of Skp2 contribute to binding cyclin A

To fully characterize how the N-terminus of Skp2 binds cyclin A, we first set out to define the minimal regions required to reconstitute the Skp2-cyclin A interaction. Using constructs of cyclins A and E encompassing only the cyclin domain (residues 173–432 and 96–378 respectively) we found that GST-tagged full-length Skp2 (GST-$Skp2^{1-424}$) pulled down CDK2-cyclin $A^{173-432}$ in both the presence or absence of Cks1 (Figure 1B, compare lanes 1 and 2). In contrast, GST-$Skp2^{1-424}$ could only pull down CDK2-cyclin E^{96-378} when Cks1 was present (lanes 3 and 4). Confirming the essentiality of the Skp2 N-terminus for direct CDK2-cyclin A binding, Skp2 lacking the first 88 residues ($Skp2^{\Delta 1-88}$) could not bind CDK2-cyclin A in the absence of Cks1 (Figure 1B, compare lanes 5/6 to lanes 1/2.)

GST-Skp2$^{1-424}$ could also pull down cyclin A in isolation but not CDK2 in isolation (Figure 1C) confirming that cyclin A was the direct interaction target of Skp2. These experiments also served to localize the Skp2 interaction region of cyclin A to the cyclin domain (173–432). Similar findings were observed recently by Salamina et al., 2021.

To localize regions within the N-terminus of Skp2 required for binding to cyclin A, we generated a series of N-terminal deletions in Skp2 and tested their ability to bind GST:CDK2-cyclin A in a pull down experiment (Figure 1D). Deletion of residues 1 to 16 of Skp2 (Skp2$^{\Delta 1-16}$) had no effect on CDK2-cyclin A binding. In contrast, deletion of amino acids 1 to 28 (Skp2$^{\Delta 1-28}$) caused a decrease in CDK2-cyclin A binding. These results localized a binding element within residues 17 to 28 (referred to as Motif 1) of Skp2. Weak binding to CDK2-cyclin A persisted until nearly the entire N-terminus of Skp2, namely residues 1 to 88, was removed. This result suggested the presence of a second cyclin A binding element in Skp2 located within residues 75 to 88 (referred to as Motif 2). Consistent with a sufficiency for binding to cyclin A, Skp2$^{17-85}$ was able to co-purify with cyclin A by size-exclusion chromatography (Figure 2A). Together, our analysis identified minimally two CDK2-cyclin A binding elements in the N-terminus of Skp2 encompassing residues 17 to 85 (see Figure 1E schematic for summary).

Structure analysis of a Skp2$^{17-84}$:GSG:cyclin A$^{173-432}$ fusion

To visualize how Skp2 binds directly to cyclin A we set out to solve a crystal structure of the N-terminus of Skp2 bound to cyclin A. When a complex of the two proteins failed to produce protein crystals, we engineered a set of fusion proteins that linked Skp2$^{17-84}$ to either the N- or C- terminus of cyclin A$^{173-432}$ through a flexible GSG, GSGSG or GSGSGSG linker. Fusions of Skp2$^{17-84}$ linked to the N-terminus of cyclin A$^{173-432}$ expressed well and the Skp2$^{17-84}$:GSG:cyclin A$^{173-432}$ fusion protein (Figure 2B) readily crystallized yielding a 3.2 Å data set. The crystal structure was solved by molecular replacement using the cyclin domain of cyclin A (PDB=1FIN) as a search model (See Table 1 for data collection and refinement statistics).

After building of a complete model of cyclin A, |Fo-Fc| electron density maps revealed two unaccounted for regions of density, which we attributed to Skp2; one along the α2-α3 loop and helix α5 of cyclin A (denoted Surface 1) and the other along the hydrophobic patch of cyclin A formed by helices α1, α3, and α4 (denoted Surface 2) (Figure 2C). Surface 2 density was unambiguously identified as residues 79 to 84 (denoted Skp2$^{79-84}$) based on side chain features and the presence of continuous density linking it to the N-terminus of cyclin A (Figure 2D). These residues correspond to interaction Motif 2 of Skp2 delineated by deletion analysis (Figure 1D).

Surface 1 density along the α2-α3 loop and helix α5 of cyclin A could not be assigned to specific residues in Skp2 due to the absence of side chain features and a lack of connectivity to known structural elements. Hence this region of Skp2 was modeled as a poly alanine chain (the directionality of the density also remains in question). We attribute this region of unaccounted density to interaction Motif 1 of Skp2 delineated by deletion analysis (Figure 1D). The final refined Skp2$^{17-84}$:GSG:cyclin A$^{173-432}$ structure contains two Skp2-cyclin

A complexes in the asymmetric unit with the Skp2$^{17-84}$ region of one polypeptide chain associating in trans with the cyclin domain of a crystallographic symmetry mate.

Skp2$^{79-84}$ (Motif 2) contains a reverse RxL motif that binds the cyclin A hydrophobic patch

Interestingly, Skp2$^{79-84}$ (corresponding to the sequence ^{79}FVIVRR^{84}) binds to the same surface of cyclin A that binds RxL motifs in CDK substrates and regulators (Brown et al., 1999; Lowe et al., 2002; Russo et al., 1996; Schulman et al., 1998) (Figure 3A). However, the sequence of Skp2$^{79-84}$ lacks an obvious RxL motif. Furthermore, in contrast to the canonical RxL motif binding mode, Skp2$^{79-84}$ binds across the hydrophobic patch in a reverse orientation (C' to N' versus N' to C'). Despite this reversed orientation, superimposition of Skp2$^{79-84}$ onto the representative RxL motif structure of p27 (^{30}RNLFG^{34}) revealed a striking similarity in the two ligand binding modes (Figure 3B). Specifically, residues with similar physiochemical properties occupied the same positions within the binding pocket (namely F79^{Skp2} vs F33^{p27}, I81^{Skp2} vs L32^{p27}, and R83^{Skp2} vs R30^{p27}). Thus Skp2$^{79-84}$ conforms to the hydrophobic patch binding consensus but in an opposite orientation (see Figure 3C for alignments). For this reason, we describe Skp2$^{79-84}$ as a reverse RxL motif.

To validate that the interactions observed in the crystal structure of the Skp2$^{17-84}$:GSG:cyclin A$^{173-432}$ fusion are relevant for the molecular interaction of isolated proteins in solution, we employed site directed mutagenesis and a fluorescence polarization binding assay using fluorescein labeled peptides (Figure 3D). Consistent with the predicted binding mode, fluorescein labeled Skp2$^{77-86}$, corresponding to interaction Motif 2, bound to wild-type CDK2-cyclin A with a K_d of 3.2 μM. Mutations of the RxL binding pocket residues including M210A/I213A, E220R, and Q254A, had varying effects on Skp2$^{77-86}$ binding; mutations E220R and Q254A abolished detectable binding of Skp2$^{77-86}$ to CDK2-cyclin A, while the M210A/I213A mutation had a more modest effect and reduced binding affinity by ~5 fold, similar to control mutations M246K, and L297K remote from the hydrophobic patch.

For comparison, we also tested the effect of the cyclin A mutations on binding to the canonical RxL motif in p27. FITC-p27$^{27-36}$ bound to wild-type CDK2-cyclin A with a K_d of 5.5 μM. As observed for the reverse RxL peptide of Skp2, the Q254A mutation abolished binding to FITC-p27$^{27-36}$, whereas the E220R mutation strongly inhibited binding. Unlike what was observed for the reverse RxL peptide of Skp2, the M210A/I213A mutation in cyclin A abolished binding to FITC-p27$^{27-36}$. Thus, while both the reverse and canonical RxL peptides bind to the same hydrophobic patch on cyclin A, the subtle differences in their binding modes leave them differentially sensitive to surface mutations.

To validate the importance of the reverse RxL motif in full length Skp2 for binding to cyclin A, we introduced the multi-site mutation F79A/I81A/R83A into full length Skp2 and tested if for its ability to displace the FITC-p27$^{27-36}$ probe from cyclin A (Figure 3E). Whereas wild-type Skp2 competitively displaced FITC-p27$^{27-36}$ from cyclin A with an IC_{50} of 5.3 μM, the reverse RxL mutant (F79A/I81A/R83A) was greatly compromised for this function (IC_{50} not determinable). Taken together, these mutational analyses prove the existence of

a physical interaction between Motif 2 in Skp2 and the hydrophobic patch (Surface 2) of cyclin A in solution.

Residues 17 to 43 in Skp2 harbours binding Motif 1 for Surface 1 of cyclin A.

As noted, a lack of side chain density prevented accurate assignment of Skp2 sequence to the unaccounted-for density along Surface 1 of cyclin A (Figure 4A). However, based on our deletion analysis (Figure 1D,E) we reasoned that the density could correspond to residues 17 to 28 of Skp2.

To probe the boundaries of Motif 1 in Skp2 further, we made progressive deletions starting from the C-terminal end of $Skp2^{1-94}$ and tested binding to CDK2-cyclin A^{1-432} using a GST pull-down assay (Figure 4B upper panel). A major loss of binding to CDK2-cyclin A was observed for $Skp2^{1-29}$ but not $Skp2^{1-43}$ and longer constructs. Consistent with our original deletion analysis, removal of the first 16 residues ($Skp2^{17-43}$) did not affect binding to CDK2-cyclin A, but deletion of the first 27 residues of this construct ($Skp2^{28-43}$) did abolish binding (Figure 4B lower panel). Together these results suggested that an important binding determinant in Skp2 for CDK2-cylin A lies between residues 17 and 43 (see Figure 4C for summary).

To determine if $Skp2^{17-43}$ (Motif 1) engages interaction Surface 1 of cyclin A, we mutagenized cyclin A and examined binding using a fluorescence polarization binding assay (Figure 4D). FITC-$Skp2^{17-43}$ bound to wild-type CDK2-cyclin A with a K_d of 3.1 μM. Three mutations on Surface 1 of cyclin A, namely K202A/Q203A, M246K, and L297K, greatly reduced binding to FITC-$Skp2^{17-43}$. In contrast, control mutations on the hydrophobic patch (Surface 2) of cyclin A (M210A/I213A, E220R, and Q254A) had negligible effect on binding. Together, these results support the notion that $Skp2^{17-43}$ (Motif 1) engages interaction Surface 1 of cyclin A.

Multiple sequence alignment of the N-terminus of Skp2 across species demonstrated a similar degree of conservation across residues 17 to 43 (Figure S1). However, previous work showed that the combined mutation of residues L32, L33, S39, and L41 in Skp2 to alanine, was sufficient to abolish the co-immunoprecipitation of full length Skp2 to CDK2-cyclin A in cells (Ji et al. 2006). We introduced the same multi-site mutations (referred to as 4A) into Skp2 residues 17 to 45 ($Skp2^{17-45}$) and measured the ability to displace FITC-$Skp2^{17-43}$ from CDK2-cyclin A *in vitro*. While wild-type $Skp2^{17-45}$ could displace FITC-labelled $Skp2^{17-43}$ with an IC_{50} of 17.8 μM, the 4A mutant of $Skp2^{17-45}$ was completely compromised for this function (Figure 4E). We next introduced the same multi-site mutations into full-length $Skp2^{1-424}$ and measured the ability to displace the FITC-$p27^{27-36}$ from CDK2-cyclin A *in vitro*. While wild-type $Skp2^{1-424}$ could displace FITC-$p27^{27-36}$ with an IC_{50} of 5.8 μM, the 4A mutant of $Skp2^{1-424}$ was 3-fold less effective at this function (IC_{50} of 17.8 μM versus 5.8 μM for the mutant and wild-type respectively) (Figure 4F). These results are consistent with the presence of partially redundant bi-partite binding elements in the Skp2 N-terminus for cyclin A with L32, L33, S39, and L41 residues of Skp2 likely residing in binding Motif 1.

Skp2 preference for binding cyclin A over cyclin E is mediated by both Motif1 and Motif 2

The N-terminus of Skp2 selectively binds CDK2-cyclin A and not CDK2-cyclin E (Figure 1B). Sequence alignments of human cyclin A and cyclin E revealed a high conservation of Surface 2 residues (i.e. hydrophobic patches, 85% identical) and a much lower conservation of Surface 1 residues (25% identical). (Figure 5A). Thus, we reasoned that specificity of Skp2 binding might be related to Motif 1 rather than Motif 2. Surprisingly, neither FITC-Skp2$^{17-43}$ (Motif 1) nor FITC-Skp2$^{77-87}$ (Motif 2, reverse RxL) detectably bound to CDK2-cyclin E complexes (Figure 5B). Thus, the specificity of the Skp2 N-terminus for cyclin A over cyclin E is attributable to the action of both interaction Motifs 1 and 2, despite near identical compositions of interaction Surface 2 residues on cyclin A and cyclin E.

Interestingly, the RxL peptide of p27 bound more tightly to CDK2-cyclin E complexes than CDK2-cyclin A complexes (K_d 0.14 μM versus 2.1 μM) (Figure 5C). This observation further highlighted how near identical binding surfaces on cyclin A and cyclin E confer surprisingly different binding specificities for ligands.

Both Motifs 1 and 2 in Skp2 compete with elements in p27 for binding to CDK2-cyclin A

Ji et al. (2006) previously showed that the N-terminus of Skp2 competes with p27 for binding to CDK2-cyclin A complexes in cell extracts. In agreement with this report, p27 could compete with Skp2 for binding to Cdk2-cyclin A in a GST pull down assay in vitro (Figure 6A). Superimposition of the Skp2$^{17-84}$:GSG:cyclin A structure onto the structure of the p27$^{25-93}$-CDK2-cyclin A complex (PDB 1JSU) revealed that this competitive binding likely occurs due to the binding of p27 and Skp2 to both Surfaces 1 and 2 of cyclin A (Figure 6B). In support, both full-length p27 and Skp2$^{17-85}$ could competitively displace FITC-labeled probes for Surface 2 (p27 RxL motif; IC_{50} = 5.2 μM and 5.1 μM respectively) and for Surface 1 (Skp2$^{17-43}$; IC_{50} = 12.0 μM and 13.4 μM respectively) (Figure 6C). Previous studies using isothermal calorimetry (ITC) showed that the kinase inhibitory domain of p27 (residues 22 to 105) binds to CDK2-cyclin A with low nanomolar binding constants (K_d=3.5 nM, Lacy et al., 2004; K_d=4.9 nM, Tsytlonok et al., 2019). ITC analysis of Skp2 N-terminus binding to CDK2-cyclin A revealed a K_d of 496 nM (Figure 6D). This 100-fold weaker binding affinity to CDK2-cyclin A suggests that the N-terminus of Skp2 is unlikely to displace p27 from CDK2-cyclin A complexes and therefore will only engage CDK2-cyclin A in the absence of p27.

Binding of Skp2 to cyclin A effectively reduces phosphorylation of CDK2-cyclin A kinase substrates containing RXL motifs

p27 binds to CDK2-cyclin A and represses its activity through two distinct mechanisms; first, by occluding the hydrophobic patch of cyclin A, which prevents the recruitment of RxL containing substrates, and second by direct inhibitory interactions with kinase domain of CDK2 (Russo et al., 1996; Vlach et al., 1997). Previously, Ji et al. (2006) found that both full-length GST-Skp2$^{1-424}$ and Skp2$^{1-88}$ could inhibit CDK2-cyclin A phosphorylation of the native substrate Rb with IC_{50} values of 520 nM and 180 nM, respectively. Since the N-terminus of Skp2 binds primarily to cyclin A and not CDK2, we reasoned that the inhibitory effect of Skp2 on Rb phosphorylation was likely due to competition for binding to cyclin A. We confirmed similar findings using the CDK1/2-cyclin A substrate Bora (Thomas

et al., 2016; Vigneron et al., 2018), which contains two RxL motifs (Figure 7A). Wild-type Skp2 could also completely inhibit Bora phosphorylation *in vitro* in a manner dependent on its N-terminus, similar to the control p27 protein. However, the higher binding affinity of p27 relative to Skp2 for Bora resulted in very different potencies (complete inhibition at 10 nM for p27 versus 10 μM $Skp2^{1-424}$).

We also assessed the inhibitory effect of p27 and Skp2 on the ATPase activity of CDK2-cyclin A measured in the absence of an RxL containing substrate. Here only p27 was able to completely repress CDK2-cyclin A activity, likely reflecting the fact that direct binding interactions of p27 and Skp2 with cyclin A have little effect on the ATPase activity of Cdk2. In contrast, p27 makes direct inhibitory interactions with the kinase domain of CDK2 (Figure 7B). These results further support the conclusion that the inhibitory effect of Skp2 on CDK2-cyclin A kinase activity is primarily due to competition for substrate binding to the hydrophobic patch on cyclin A.

Discussion

We sought to uncover the molecular basis for the interaction of the N-terminus of Skp2 with CDK2-cyclin A. By fusing the minimal regions required for complex formation, namely $Skp2^{17-84}$ and cyclin $A^{173-432}$, with a short flexible linker, we were able to crystallize and solve a structure that revealed a bi-partite mode of interaction. The structure identifies two surfaces on cyclin A involved in binding to the N-terminus of Skp2; first, the hydrophobic patch formed by helices α1, α3, and α4 (Surface 2) and second a distinct surface formed by the α2-α3 loop and helix α5 (Surface 1). Additionally, the structure revealed Skp2 residues 79 to 84 as the cyclin A binding motif (Motif 2) that engages the hydrophobic patch. The second cyclin A binding motif could not be unambiguously identified but appears contained within Skp2 residues 17 to 43 (Motif 1). Our analyses also revealed that Motif 1 and Motif 2 in Skp2 selectively bind to CDK2-cyclin A and not CDK2-cyclin E complexes. The specificity of cyclin A binding Motif 2 was particularly surprising because of the strong conservation of residues on Surface 2 between cyclin A and cyclin E proteins. Lastly, the crystal structure explains the basis for competition between Skp2 and p27 for binding to cyclin A. This competitive binding mode allows the N-terminus of Skp2 to inhibit CDK2-cyclin A phosphorylation of RxL containing substrates such as Rb and Bora but is unlikely to affect phosphorylation of substrates recruited to CDK2-cyclin A through alternate mechanisms.

The crystal structure of the Skp2:cyclin A fusion complex is consistent with recently published work. Using HDX-MS, Salamina et al. (2021) uncovered an elongated interaction surface on cyclin A for the N-terminus of Skp2 that contains both Surfaces 1 and 2 revealed by our crystallographic analysis. In the HDX-MS analysis, a loop region in cyclin A corresponding to residues 201 to 209 was identified as composing part of Skp2 binding surface (Figure 8). This loop provides a hint into the possible connectivity between Skp2 Motifs 1 and 2. The simplest connectivity model would be one in which Motif 1 and Motif 2 bind in an anti-parallel manner such that the intervening linker binds across the cyclin A $loop^{201-209}$. Even with this constraint, the precise sequence of Skp2 residues comprising the electron density of Motif 1 in our crystal structure remains in question.

Our work and others have demonstrated that multi-site mutation of residues L32, L33, S39, and L41 disrupts binding to cyclin A (Ji et al., 2006; Salamina et al., 2021). In the hypothetical antiparallel binding mode, these residues, which are embedded in the conserved and hydrophobic sequence ^{32}LLSGMGVSAL^{41}, would be well placed to interact favourably with the hydrophobic properties of Surface 1. Interestingly, a similar surface on the budding yeast cyclins Cln1 and Cln2 has been implicated in binding short linear motifs containing hydrophobic amino acids, particularly Leu and Pro (Figure 8B) (Bandyopadhyay et al., 2020; Bhaduri et al., 2015). Further work will be required to validate these inferences.

Our finding that Motif 2 (^{79}FVIVRR^{84}) of Skp2 interacts with the cyclin A hydrophobic patch (Surface 2) has interesting implications for CDK substrate recognition. Cyclins A, B, D1, and E each have a highly similar hydrophobic patch surface that can recognize RxL motifs (either (K/R)xLΦ or (K/R)xLxΦ, where x is any residue and Φ is a large hydrophobic residue) within their substrates and intermolecular regulators (Adams et al., 1996; Chen et al., 1996; Guiley et al., 2019; Russo et al., 1996). Subtle differences in sequence within and preceding the RxL motif and on the complementary hydrophobic patch imparts a measure of selectivity in substrate recognition (Brown et al., 2007; Örd et al., 2020; Wohlschlegel et al., 2001). The discovery that a non-RxL sequence within the N-terminus Skp2 can bind the hydrophobic patch of cyclin A raises the possibility that the hydrophobic patch of each cyclin could bind a larger number of short linear motifs than previously appreciated. Indeed, a number of short non-RxL containing linear motifs have been identified as hydrophobic patch binders to the B-type cyclins in budding yeast (Faustova et al., 2021; Örd et al., 2020). Our work provides a possible model for how proteins lacking apparent RxL motifs bind to cyclins.

Finally, how might the interaction of the N-terminus of Skp2 and cyclin A affect the biological function of these two proteins? It is well appreciated that the LRR domain of Skp2 binds CDK2-cyclin A complexes via Cks1 to promote the ubiquitination of p27 (Figure 8C, top). By comparison, the biological function of CDK2-cyclin A binding to the N-terminus of Skp2 is poorly understood. Our work reveals that the N-terminus of Skp2 occupies the canonical substrate-binding surface on cyclin A and can therefore exert a complete inhibitory effect on CDK2 phosphorylation of RxL containing substrates *in vitro* (Figure 8C, bottom). Interestingly, the binding of Skp2 to cyclin A has only a partial inhibitory effect on the intrinsic kinase activity of CDK2, which raises the possibility that CDK2-cyclin A bound to the N-terminus of Skp2 could still phosphorylate proteins present in close vicinity. In this way, rather than inhibiting CDK2-cyclin A, binding to the Skp2 N-terminus could re-direct kinase activity towards an alternate set of substrates lacking RxL motifs. The N-terminus of Skp2 is also implicated in binding other targets and thus binding to cyclin A may reciprocally inhibit their engagement. Whether this is the case for Skp2 binding to Cdh1 or Rb remains to be determined. We posit that the knowledge gained from the crystal structure presented here will provide a platform for future studies aimed at dissecting the different biological functions of the Skp2 N-terminus.

STAR Methods

RESOURCE AVAILABILITY

Lead contact—Further information and requests for resources and reagents should be directed to and will be fulfilled by the lead contact, Frank Sicheri (sicheri@lunenfeld.ca).

Materials availability statement—Materials generated in this study can be made available upon request from the Lead contact.

Data and code availability—The accession number for the Skp2$^{17-84}$:GSG:cyclin A$^{173-432}$ coordinates and structure factors reported in this paper is Protein Data Bank: 7LUO.

EXPERIMENTAL MODEL AND SUBJECT DETAILS

Bacterial cell culture—Cloning was performed using *Escherichia coli* DH5alpha cells. Protein expression was performed using *Escherichia coli* BL21 (DE3) cells. For both strains, cells transformed with plasmid were grown in either LB or TB media containing a 100 mg/mL ampicillin at 37°C. For protein expression 1L cultures were grown shaking at 200 rpm and 37°C to an OD_{600} of 0.8 to 1 before inducing protein expression with 0.5 mM IPTG and incubating cultures at 18°C overnight.

METHOD DETAILS

Cloning and plasmid construction—The pGEX 4T-3 plasmid co-expressing human CDK2 residues 1–298 (GST-tagged, Prescission protease cleavable, sequence verified) and *Saccharomyces cerevisiae* CAK1 (GST-tagged, non-cleavable) was a gift from Tanja Mittag (St. Jude Children's Research Hospital). All other constructs were cloned into either pGEX or pProEX plasmids using classical restriction enzyme cloning (primers listed in Table S1). For co-expression of Skp2 with Skp1, the 6XHis-tagged Skp1 crystallography construct (1–163, Δ38–43, Δ70–77, K78G E79S K80G R81G) in the pProEX vector was cut with SspI and inserted into the Skp2-pGEX vector at the StuI site by blunt ended ligation. The Skp2$^{17-84}$-GSG-cyclin A$^{173-432}$ fusion protein was created using overlap extension PCR to fuse Skp2$^{17-84}$ to cyclin A$^{173-432}$ separated by the GSG linker (primers indicated in the Key Resource Table). NcoI and SacI restriction enzyme cut sites were added to the N- and C-terminus (respectively) by PCR, allowing for insertion of the fusion protein coding region into the pGEX expression vector.

Protein expression and purification—Cyclin A (either residues 1–432 or 173–432) was expressed as a TEV cleavable N-terminal 6XHis fusion protein. Bacterial pellets were lysed in buffer containing 25 mM HEPES pH 7.5, 400 mM NaCl, 20 mM imidazole, 10% glycerol, 2 mM β-mercaptoethanol, and 2 mM PMSF. Cleared lysates were passed over a 5 mL HiTrap Ni-chelation column (GE LifeScience Inc.), and were eluted using a gradient from 20 mM to 500 mM imidazole. Fractions containing cyclin A were pooled and dialyzed against a buffer of 25 mM HEPES pH 7.5, 400 mM NaCl and 2 mM β-mercaptoethanol overnight at 4°C in the presence of 500 μg non-cleavable 6XHis tagged TEV protease. Dialyzed protein was then passed over a 5 mL HiTrap Ni-chelation column to remove TEV

and the cleaved 6XHis-tag. Finally, cyclin A was concentrated and loaded onto a Superdex S75 sizing column equilibrated in buffer containing 25 mM HEPES pH 7.5, 400 mM NaCl, and 1 mM DTT.

CDK2 (residues 1–298) was expressed as a PreScission protease cleavable N-terminal GST fusion protein. Bacterial pellets were lysed in buffer containing 25 mM HEPES pH 7.5, 250 mM NaCl, 10% glycerol, 2 mM β-mercaptoethanol and 2 mM PMSF. Cleared lysates were then passed over glutathione Sepharose resin (GE LifeScience Inc.) and eluted by incubation with 1 mg non-cleavable GST-PreScission protease overnight at 4°C. Eluted CDK2 was concentrated and loaded onto a Superdex S75 column equilibrated in buffer containing 25 mM HEPES pH 7.5, 250 mM NaCl, and 1 mM DTT.

CDK2-cyclin A complexes were formed by combining bacteria pellets expressing either GST-CDK2 or 6XHis-cyclin A. Pellets were combined in a ratio of 1:1 and resuspended in lysis buffer containing 25 mM HEPES pH 7.5, 400 mM NaCl, 20 mM imidazole, 10% glycerol, 2 mM β-mercaptoethanol, and 2 mM PMSF. Similar to cyclin A above, cleared lysates were passed over a 5 mL HiTrap Ni-chelation column (GE LifeScience Inc.) and eluted using a gradient from 20 mM to 500 mM imidazole. Fractions containing CDK2-cyclin A were combined and then passed over glutathione Sepharose resin (GE LifeScience Inc.). CDK2-cyclin A complexes were then released by incubation with 1 mg GST-PreScission protease and 500 μg 6XHis-TEV overnight at 4°C. Following tag cleavage, the complex was passed over a 5 mL HiTrap Ni-chelation column to removed 6XHis-TEV and the cleaved 6XHis-tag. After concentrating, the 1:1 complex was loaded onto a Superdex S75 column equilibrated in a buffer containing 25 mM HEPES pH 7.5, 400 mM NaCl, and 1 mM DTT. The CDK2-cyclin E (residues 96–378) complex was purified using the method described for CDK2-cyclin A.

Cks1 (residues 1–79) was expressed as a TEV cleavable N-terminal GST fusion protein. Bacterial pellets were lysed in buffer containing 25 mM HEPES pH 7.5, 250 mM NaCl, 10% glycerol, 2 mM β-mercaptoethanol, and 2 mM PMSF. Cleared lysates were then passed over glutathione Sepharose resin (GE LifeScience Inc.) and eluted by incubation with 500 μg 6XHis-TEV overnight at 4°C. Eluted Cks1 was then passed over a 1 mL HiTrap Ni-chelation column (GE LifeScience Inc.) to remove His-TEV. Cks1 was finally concentrated and loaded onto a Superdex S75 column equilibrated in a buffer containing 25 mM HEPES pH 7.5, 250 mM NaCl, and 1 mM DTT.

Skp1 (crystallography construct from Schulman et al., 2000) and Skp2 (all constructs containing residues 89–424) constructs were expressed together as TEV cleavable 6XHis and GST fusions, respectively. Bacterial pellets were resuspended and lysed in buffer containing 25 mM HEPES pH 7.5, 250 mM NaCl, 20 mM imidazole, 10% glycerol, 2 mM β-mercaptoethanol, and 2 mM PMSF. Skp1-Skp2 complexes were affinity purified as described for CDK2-cyclin A prior to tag cleavage. Skp1-Skp2 were eluted from glutathione Sepharose resin (GE LifeScience Inc.) by incubation with 500 μg 6XHis-TEV overnight at 4°C. Eluted Skp1-Skp2 was diluted into a buffer containing 25 mM HEPES pH 7.5, 50 mM NaCl, and 1 mM DTT. Skp1-Skp2 protein was then loaded onto a 5 mL Q-column and then eluted using a 50 mM to 500 mM NaCl gradient. Fractions containing pure Skp1-Skp2 were

combined, concentrated, and loaded onto a Superdex S75 column equilibrated in a buffer containing 25 mM HEPES pH 7.5, 250 mM NaCl, and 1 mM DTT.

The Skp2 N-terminus (residues 17–45 and 17–85) was expressed as a TEV cleavable N-terminal GST fusion protein and was purified using the method described for GST-Cks1.

p27 (residues 1–198) was expressed as a TEV cleavable N-terminal 6XHis fusion protein. Bacterial pellets were lysed in buffer containing 25 mM HEPES pH 7.5, 250 mM NaCl, 20 mM imidazole, 10% glycerol, 2 mM β-mercaptoethanol, and 2 mM PMSF. Cleared lysates were loaded onto a 5 mL HiTrap Ni-chelation column (GE LifeScience Inc.), and eluted using a gradient from 20 mM to 500 mM imidazole. Fractions containing p27 were pooled and dialyzed against a buffer containing 25 mM HEPES pH 7.5, 50 mM NaCl and 2 mM β-mercaptoethanol overnight at 4°C in the presence of 500 μg 6XHis-TEV protease. Dialyzed protein was then passed over a 5 mL Q-column. Flow-through containing p27 protein was concentrated and loaded onto a Superdex S75 column equilibrated in a buffer containing 25 mM HEPES pH 7.5, 150 mM NaCl, and 1 mM DTT.

The Skp2$^{17-84}$-GSG-cyclin A$^{173-432}$ fusion protein was expressed as a TEV cleavable N-terminal GST fusion protein. Fusion protein was purified using the described for GST-Cks1 using a buffer containing 25 mM HEPES pH 7.5, 400 mM NaCl, 10% glycerol, 2 mM DTT, and 2 mM PMSF at the cell lysis step. The final SEC buffer contained 25 mM HEPES pH 7.5, 400 mM NaCl, 10% glycerol, and 2 mM DTT.

Crystallography—Crystals of Skp2$^{17-84}$:GSG:cyclin A$^{173-432}$ were grown in sitting drop 96-well plates by mixing 0.5 μL of a solution containing 160 μM protein with 0.5 μL well solution (1.7 M NaH_2PO_4/K_2HPO_4, pH 6.2) at 20°C. For cryoprotection, crystals were soaked in well solution supplemented with 25% ethylene glycol. Diffraction data was collected from a single frozen crystal at 0.97918 Å wavelength on beamline NE-CAT (APS, Chicago, Il) and processed with XDS (Kabsch, 2010). Molecular replacement was performed using Phaser (McCoy et al., 2007) and with the structure of cyclin A (PDB: 1FIN) as a search model. Refinement was performed using PHENIX (Adams et al., 2011) with TLS parameters and torsion-angle NCS on. Model building was done in Coot (Emsley et al., 2010). Software used in this project was curated by SBGrid (Morin et al., 2013). X-ray data collection and refinement statistics are shown in Table 1. Final structure consists of two Skp2$^{17-84}$:GSG:cyclin A$^{173-432}$ complexes in the asymmetric unit.

GST pull down experiments—CDK2-cyclin A and Skp1-Skp2 complexes purified by Nickel affinity chromatography were immobilized on glutathione Sepharose resin (GE Healthcare Life Sciences). Untagged proteins were combined with resin in a total volume of 100 μL in binding buffer containing 25 mM HEPES pH 7.5, 150 mM NaCl, 1 mM DTT, and 0.01% NP-40. Following 1 hour incubation at 4°C with mild agitation, pelleted resin was washed 3 times with 500 μL of binding buffer. Resin was resuspended in sample buffer and supernatants were analyzed by SDS-PAGE.

Peptide synthesis—FITC-Skp2$^{17-43}$ was purchased from Biomatik Corporation. The peptide was resuspended in 25 mM HEPES pH 7.0 and quantified by absorbance

measurement at 493 nm using the extinction coefficient of FITC (80,000 L mol^{-1} cm^{-1}). FITC-$Skp2^{77-86}$ and FITC-$p27^{27-36}$ peptides were synthesized by solid phase peptide synthesis using 9-fluorenylmethoxycarbonyl chemistry on Rink amide MBHA resin (Novabiochem) on a Prelude peptide synthesizer (Protein Technologies, Inc.). FITC-$Skp2^{77-86}$ contains a non-native beta-alanine at the N-terminus to facilitate FITC functionalization. Peptides were deprotected in the cleavage cocktail containing trifluoroacetic acid, phenol, water, thioanisole, 1,2-ethanedithiol (82.5%:5%:5%:5%:2.5% v/v) for 90 minutes at room temperature and then precipitated in t-butyl methyl ether. Crude peptides were purified using C-18 reverse phase HPLC (Waters) and authenticity was confirmed by mass spectrometry on an Orbitrap Elite (Thermo Fisher Scientific). The N-terminus of each peptide was functionalized directly with 5-(and-6)-carboxyfluorescein (ThermoFisher Scientific). Peptides were resuspended in 20 mM HEPES pH 7.0 and concentrations were determined from absorbance measurements at 495 nm using the extinction coefficient of FITC (80,000 L mol−1 cm−1).

Fluorescence polarization assays—FITC-$Skp2^{77-86}$ and FITC-$p27^{27-36}$ peptides were synthesized in-house. Binding experiments were performed with 25 nM FITC-conjugated peptides and the indicated amount of CDK2-cyclin complex in buffer containing 25 mM HEPES pH 7.5, 150 mM NaCl, 5 mM DTT, 0.01% Brij-35 and 0.1 mg mL^{-1} BSA. The competitive displacement assay was performed using 25 nM of the indicated FITC-peptide and the indicated amount of CDK2-cyclin A (see figure legends). Concentration of non-FITC labeled competitor proteins/peptides were added to the final indicated concentrations. Mixed samples (25 μL total volume) were incubated for 30 min in 384-well, black, flat-bottom, low-flange plates (Corning, 3573). Fluorescence intensities were measured using a BioTek Synergy Neo plate reader with excitation and absorbance at 485/528 nm respectively. Fluorescence polarization was calculated with the Gen5 Data Analysis Software. Graphs and the derived binding constants were generated using GraphPad Prism v8.2.1 (GraphPad).

Isothermal Calorimetry—Calorimetric titrations were performed on a Malvern MicroCal Auto-iTC200 (SBC Facility at The Hospital for Sick Children) at 25°C. Protein samples were prepared in a buffer containing 25 mM HEPES pH 7.5, 250 mM NaCl, and 1 mM DTT. To measure binding between $Skp2^{17-85}$ and CDK2-cyclin $A^{173-432}$, 150 μM $Skp2^{17-85}$ in the syringe was titrated into 15 μM CDK2-cyclin A in the cell. A total of 19 injections were performed with 180 seconds between injections. Data was processed using Origin 7 (v7.0552).

CDK2-cyclin protein kinase and ATPase activity assays—ATPase activity of purified CDK2-cyclin $A^{173-432}$ was measured using the ADP-Glo Kinase assay kit (Promega) as per manufacturer's instructions. Each 20 μL reaction contained 3 nM CDK2-cyclin A, with $p27^{1-198}$, Skp1-$Skp2^{1-424}$ (full-length) or $Skp2^{17-85}$ (N-terminus) at the indicated concentrations in buffer containing 40 mM Tris pH 7.5, 50 mM NaCl, 10 mM $MgCl_2$, 2 mM $MnCl_2$, 0.1 mg mL^{-1} BSA, 0.01% Brij 35, and 1 mM DTT. Reactions were initiated by adding ATP (10 μM final) and then incubated at room temperature (20°C) for 60 minutes. Reactions were terminated by transferring 10 μL of the reaction mix to a 384

well white plate (Lumitrac 200, VWR) containing 10 μL of ADP-Glo™ Reagent. Sample plates were incubated at room temperature for 40 minutes after which 20 μL of kinase detection reagent was added. Following incubation at room temperature for 30 minutes, luminescence was measured on a BioTek Synergy Neo plate reader (BioTek) with Gen5 v2.05 software using a 1 second integration time. Results were plotted in GraphPad Prism v8.2.1 (GraphPad).

Protein kinase assays measuring Bora$^{1-224}$ phosphorylation by CDK2-cyclin A were performed in a buffer containing 25 mM HEPES pH 7.5, 150 mM NaCl, 1 mM DTT, 0.75 mM ATP, and 1.5 mM $MgCl_2$. Each 10 μL reaction contained 10 μCi of ATP [γ-^{32}P], 3 nM CDK2-cyclin A$^{173-432}$ and 10 μM Bora$^{1-224}$. Where indicated, p27$^{1-198}$, Skp1-Skp2$^{1-424}$ (full-length), Skp1-Skp2 $^{\Delta 1-88}$, or Skp2$^{17-85}$ (N-terminus) were added at the concentrations specified. After incubation at 30°C for 30 minutes, reactions were terminated by the addition of sample buffer and then subjected to SDS PAGE analysis. Gels were exposed to a PhosphorImager plate for 3 hours. The plate was then scanned and visualized with a PhosphorImager (Molecular Dynamics).

QUANTIFICATION AND STATISTICAL ANALYSIS

The number of replicate experiments (N) represented by the data can be found in the individual figures and figure legends. Representative images are shown for GST pull down and radioactive kinase experiments repeated N=2 or 3 times. Fluorescence polarization binding and competition experiments were repeated N=3 or 4 times. ADP-Glo™ kinase assay was repeated N=3 times. K_d and IC_{50} values were calculated for each replicate experiment using GraphPad Prism version 8.2.1 with mean and standard deviation (SD) reported in each figure. ITC binding experiments were performed N=3 times. K_d values were calculated for each replicate using Origin 7 (v7.0552) with mean and standard deviation reported in the figure. Error bars on individual data points in all figures represent standard deviation (SD).

Supplementary Material

Refer to Web version on PubMed Central for supplementary material.

Acknowledgements

This work was supported by a CIHR foundation grant to F.S. and an NSERC PGS D to S.K. and was based upon research conducted at the Northeastern Collaborative Access Team beamlines, which are funded by the National Institute of General Medical Sciences from the National Institutes of Health (P30 GM124165). This research used resources of the Advanced Photon Source, a U.S. Department of Energy (DOE) Office of Science User Facility operated for the DOE Office of Science by Argonne National Laboratory under Contract No. DE-AC02–06CH11357. We thank Nicolas Tavernier for providing Bora protein and acknowledge The Hospital for Sick Children's Structural & Biophysical Core Facility staff and infrastructure.

References

Adams PD, Sellers WR, Sharma SK, Wu AD, Nalin CM, and Kaelin WG (1996). Identification of a cyclin-cdk2 recognition motif present in substrates and p21-like cyclin-dependent kinase inhibitors. Mol. Cell. Biol. 16, 6623–6633. [PubMed: 8943316]

Adams PD, Afonine PV, Bunkóczi G, Chen VB, Echols N, Headd JJ, Hung LW, Jain S, Kapral GJ, Grosse Kunstleve RW, et al. (2011). The Phenix software for automated determination of macromolecular structures. Methods 55, 94–106. [PubMed: 21821126]

Bandyopadhyay S, Bhaduri S, Örd M, Davey NE, Loog M, and Pryciak PM (2020). Comprehensive Analysis of G1 Cyclin Docking Motif Sequences that Control CDK Regulatory Potency In Vivo. Curr. Biol. 30, 4454–4466.e5. [PubMed: 32976810]

Bashir T, Dorello HV, Amador V, Guardavaccaro D, and Pagano M (2004). Control of the SCFSkp2-Cks1 ubiquitin ligase by the APC/C Cdh1 ubiquitin ligase. Nature 428, 190–193. [PubMed: 15014502]

Bhaduri S, Valk E, Winters MJ, Gruessner B, Loog M, and Pryciak PM (2015). A docking interface in the cyclin Cln2 promotes multi-site phosphorylation of substrates and timely cell-cycle entry. Curr. Biol. 25, 316–325. [PubMed: 25619768]

Bourne Y, Watson MH, Hickey MJ, Holmes W, Rocque W, Reed SI, and Tainer JA (1996). Crystal structure and mutational analysis of the human CDK2 kinase complex with cell cycle-regulatory protein CksHs1. Cell 84, 863–874. [PubMed: 8601310]

Brown NR, Noble MEM, Endicott JA, and Johnson LN (1999). The structural basis for specificity of substrate and recruitment peptides for cyclin-dependent kinases. Nat. Cell Biol. 1, 438–443. [PubMed: 10559988]

Brown NR, Lowe ED, Petri E, Skamnaki V, Antrobus R, and Johnson LN (2007). Cyclin B and cyclin A confer different substrate recognition properties on CDK2. Cell Cycle 6, 1350–1359. [PubMed: 17495531]

Carrano AC, Eytan E, Hershko A, and Pagano M (1999). SKP2 is required for ubiquitin-mediated degradation of the CDK inhibitor p27. Nat. Cell Biol. 1, 193–199. [PubMed: 10559916]

Chang B, Partha S, Hofmann K, Lei M, Goebl M, Harper JW, and Elledge SJ (1996). SKP1 connects cell cycle regulators to the ubiquitin proteolysis machinery through a novel motif, the F-box. Cell 86, 263–274. [PubMed: 8706131]

Chen J, Saha P, Kornbluth S, Dynlacht BD, and Dutta A (1996). Cyclin-binding motifs are essential for the function of p21CIP1. Mol. Cell. Biol. 16, 4673–4682. [PubMed: 8756624]

Emsley P, Lohkamp B, Scott WG, and Cowtan K (2010). Features and development of Coot. Acta Crystallogr. Sect. D Biol. Crystallogr. 66, 486–501. [PubMed: 20383002]

Faustova I, Bulatovic L, Matiyevskaya F, Valk E, Örd M, and Loog M (2021). A new linear cyclin docking motif that mediates exclusively S-phase CDK-specific signaling. EMBO J. 40, e105839. [PubMed: 33210757]

Feldman RMR, Correll CC, Kaplan KB, and Deshaies RJ (1997). A complex of Cdc4p, Skp1p, and Cdc53p/cullin catalyzes ubiquitination of the phosphorylated CDK inhibitor Sic1p. Cell 91, 221–230. [PubMed: 9346239]

Ganoth D, Bornstein G, Ko TK, Larsen B, Tyers M, Pagano M, and Hershko A (2001). The cell-cycle regulatory protein Cks1 is required for SCFSkp2-mediated ubiquitinylation of p27. Nat. Cell Biol. 3, 321–324. [PubMed: 11231585]

Gao D, Inuzuka H, Tseng A, Chin RY, Toker A, and Wei W (2009). Phosphorylation by Akt1 promotes cytoplasmic localization of Skp2 and impairs APCCdh1-mediated Skp2 destruction. Nat. Cell Biol. 11, 397–408. [PubMed: 19270695]

Guiley KZ, Stevenson JW, Lou K, Barkovich KJ, Kumarasamy V, Wijeratne TU, Bunch KL, Tripathi S, Knudsen ES, Witkiewicz AK, et al. (2019). P27 allosterically activates cyclin-dependent kinase 4 and antagonizes palbociclib inhibition. Science. 366.

Hochegger H, Takeda S, and Hunt T (2008). Cyclin-dependent kinases and cell-cycle transitions: Does one fit all? Nat. Rev. Mol. Cell Biol. 9, 910–916. [PubMed: 18813291]

Inuzuka H, Gao D, Finley LWS, Yang W, Wan L, Fukushima H, Chin YR, Zhai B, Shaik S, Lau AW, et al. (2012). Acetylation-dependent regulation of Skp2 function. Cell 150, 179–193. [PubMed: 22770219]

Jeffrey PD, Russo AA, Polyak K, Gibbs E, Hurwitz J, Massagué J, and Pavletich NP (1995). Mechanism of CDK activation revealed by the structure of a cyclinA-CDK2 complex. Nature 376, 313–320. [PubMed: 7630397]

Ji P, Jiang H, Rekhtman K, Bloom J, Ichetovkin M, Pagano M, and Zhu L (2004). An Rb-Skp2-p27 pathway mediates acute cell cycle inhibition by Rb and is retained in a partial-penetrance Rb mutant. Mol. Cell 16, 47–58. [PubMed: 15469821]

Ji P, Goldin L, Ren H, Sun D, Guardavaccaro D, Pagano M, and Zhu L (2006). Skp2 contains a novel cyclin A binding domain that directly protects cyclin A from inhibition by p27 Kip1. J. Biol. Chem. 281, 24058–24069. [PubMed: 16774918]

Kabsch W (2010). XDS. Acta Crystallogr. D. Biol. Crystallogr. 66, 125–132.

Komander D, and Rape M (2012). The ubiquitin code. Annu. Rev. Biochem. 81, 203–229. [PubMed: 22524316]

Lacy ER, Filippov I, Lewis WS, Otieno S, Xiao L, Weiss S, Hengst L, and Kriwacki RW (2004). p27 binds cyclin-CDK complexes through a sequential mechanism involving binding-induced protein folding. Nat. Struct. Mol. Biol. 11, 358–364. [PubMed: 15024385]

Lowe ED, Tews I, Cheng KY, Brown NR, Gul S, Noble MEM, Gamblin SJ, and Johnson LN (2002). Specificity determinants of recruitment peptides bound to phosphor-CDK2/cyclin A. Biochemistry 41, 15625–15634. [PubMed: 12501191]

McCoy AJ, Grosse-Kunstleve RW, Adams PD, Winn MD, Storoni LC, and Read RJ (2007). Phaser crystallographic software. J. Appl. Crystallogr. 40, 658–674. [PubMed: 19461840]

Montagnoli A, Fiore F, Eytan E, Carrano AC, Draetta GF, Hershko A, and Pagano M (1999). Ubiquitination of p27 is regulated by Cdk-dependent phosphorylation and trimeric complex formation. Genes Dev. 13, 1181–1189. [PubMed: 10323868]

Morin A, Eisenbraun B, Key J, Sanschagrin PC, Timony MA, Ottaviano M, and Sliz P (2013). Collaboration gets the most out of software. Elife 2013, 1–6.

Örd M, Puss KK, Kivi R, Möll K, Ojala T, Borovko I, Faustova I, Venta R, Valk E, Kõivomägi M, et al. (2020). Proline-Rich Motifs Control G2-CDK Target Phosphorylation and Priming an Anchoring Protein for Polo Kinase Localization. Cell Rep. 31.

Pettersen EF, Goddard TD, Huang CC, Couch GS, Greenblatt DM, Meng EC, and Ferrin TE (2004). UCSF Chimera - A visualization system for exploratory research and analysis. J. Comput. Chem. 25, 1605–1612. [PubMed: 15264254]

Russo AA, Jeffrey PD, Patten AK, Massagué J, and Pavletich NP (1996). Crystal structure of the p27(Kip1) cyclin-dependent-kinase inhibitor bound to the cyclin A-Cdk2 complex. Nature 382, 325–331. [PubMed: 8684460]

Salamina M, Montefiore BC, Liu M, Wood DJ, Heath R, Ault JR, Wang L-Z, Korolchuk S, Baslé A, Pastok MW, et al. (2021). Discriminative SKP2 interactions with CDK-cyclin complexes support a cyclin A-specific role in p27KIP1 degradation. J. Mol. Biol. 166795. [PubMed: 33422522]

Schulman BA, Lindstrom DL, and Harlow E (1998). Substrate recruitment to cyclin-dependent kinase 2 by a multipurpose docking site on cyclin A. Proc. Natl. Acad. Sci. U. S. A. 95, 10453–10458. [PubMed: 9724724]

Schulman BA, Carrano AC, Jeffrey PD, Browen Z, Kinnucan ERE, Finnin MS, Elledge SJ, Harper JW, Pagano M, and Pavletich NP (2000). Insights into SCF ubiquitin ligases from the structure of the Skp1-Skp2 complex. Nature 408, 381–386. [PubMed: 11099048]

Sievers F, Wilm A, Dineen D, Gibson TJ, Karplus K, Li W, Lopez R, McWilliam H, Remmert M, Söding J, et al. (2011). Fast, scalable generation of high-quality protein multiple sequence alignments using Clustal Omega. Mol. Syst. Biol. 7.

Skowyra D, Craig KL, Tyers M, Elledge SJ, and Harper JW (1997). F-box proteins are receptors that recruit phosphorylated substrates to the SCF ubiquitin-ligase complex. Cell 91, 209–219. [PubMed: 9346238]

Spruck C, Strohmaier H, Watson M, Smith APL, Ryan A, Krek W, and Reed SI (2001). A CDK-independent function of mammalian Cks1: Targeting of SCF Skp2 to the CDK inhibitor p27 Kip1. Mol. Cell 7, 639–650. [PubMed: 11463388]

Sutterlüty H, Chatelain E, Marti A, Wirbelauer C, Senften M, Müller U, and Krek W (1999). p45SKP2 promotes p27Kip1 degradation and induces S phase in quiescent cells. Nat. Cell Biol. 1, 207–214. [PubMed: 10559918]

Thomas Y, Cirillo L, Panbianco C, Martino L, Tavernier N, Schwager F, Van Hove L, Joly N, Santamaria A, Pintard L, et al. (2016). Cdk1 Phosphorylates SPAT-1/Bora to Promote Plk1 Activation in C. elegans and Human Cells. Cell Rep. 15, 510–518. [PubMed: 27068477]

Tsvetkov LM, Yeh KH, Lee SJ, Sun H, and Zhang H (1999). p27(Kip1) ubiquitination and degradation is regulated by the SCF(Skp2) complex through phosphorylated Thr187 in p27. Curr. Biol. 9, 661–664. [PubMed: 10375532]

Tsytlonok M, Sanabria H, Wang Y, Felekyan S, Hemmen K, Phillips AH, Yun MK, Waddell MB, Park CG, Vaithiyalingam S, et al. (2019). Dynamic anticipation by Cdk2/Cyclin A-bound p27 mediates signal integration in cell cycle regulation. Nat. Commun. 10.

Vigneron S, Sundermann L, Labbé JC, Pintard L, Radulescu O, Castro A, and Lorca T (2018). Cyclin A-cdk1-Dependent Phosphorylation of Bora Is the Triggering Factor Promoting Mitotic Entry. Dev. Cell 45, 637–650.e7. [PubMed: 29870721]

Vlach J, Hennecke S, and Amati B (1997). Phosphorylation-dependent degradation of the cyclin-dependent kinase inhibitor p27 Kip1. EMBO J. 16, 5334–5344. [PubMed: 9311993]

Waterhouse AM, Procter JB, Martin DMA, Clamp M, and Barton GJ (2009). Jalview Version 2-A multiple sequence alignment editor and analysis workbench. Bioinformatics 25, 1189–1191. [PubMed: 19151095]

Wei W, Ayad NG, Wan Y, Zhang GJ, Kirschner MW, and Kaelin WG (2004). Degradation of the SCF component Skp2 in cell-cycle phase G1 by the anaphase-promoting complex. Nature 428, 194–198. [PubMed: 15014503]

Wohlschlegel JA, Dwyer BT, Takeda DY, and Dutta A (2001). Mutational Analysis of the Cy Motif from p21 Reveals Sequence Degeneracy and Specificity for Different Cyclin-Dependent Kinases. Mol. Cell. Biol. 21, 4868–4874. [PubMed: 11438644]

Yam CH, Ng RWM, Yi Siu W, Lau AWS, and Poon RYC (1999). Regulation of Cyclin A-Cdk2 by SCF Component Skp1 and F-Box Protein Skp2. Mol. Cell. Biol. 19, 635–645. [PubMed: 9858587]

Zhang H, Kobayashi R, Galaktionov K, and Beach D (1995). p19skp1 and p45skp2 are essential elements of the cyclin A-CDK2 S phase kinase. Cell 82, 915–925. [PubMed: 7553852]

Highlights:

- The N-terminus of Skp2 contains two separate cyclin A binding motifs
- Skp2 binds to a surface on cyclin A known to bind ‘RxL’ motifs
- Skp2 contains a reverse ‘RxL’ motif that binds cyclin A but not cyclin E
- Skp2 binding to cyclin A blocks recruitment of RxL-containing CDK substrates

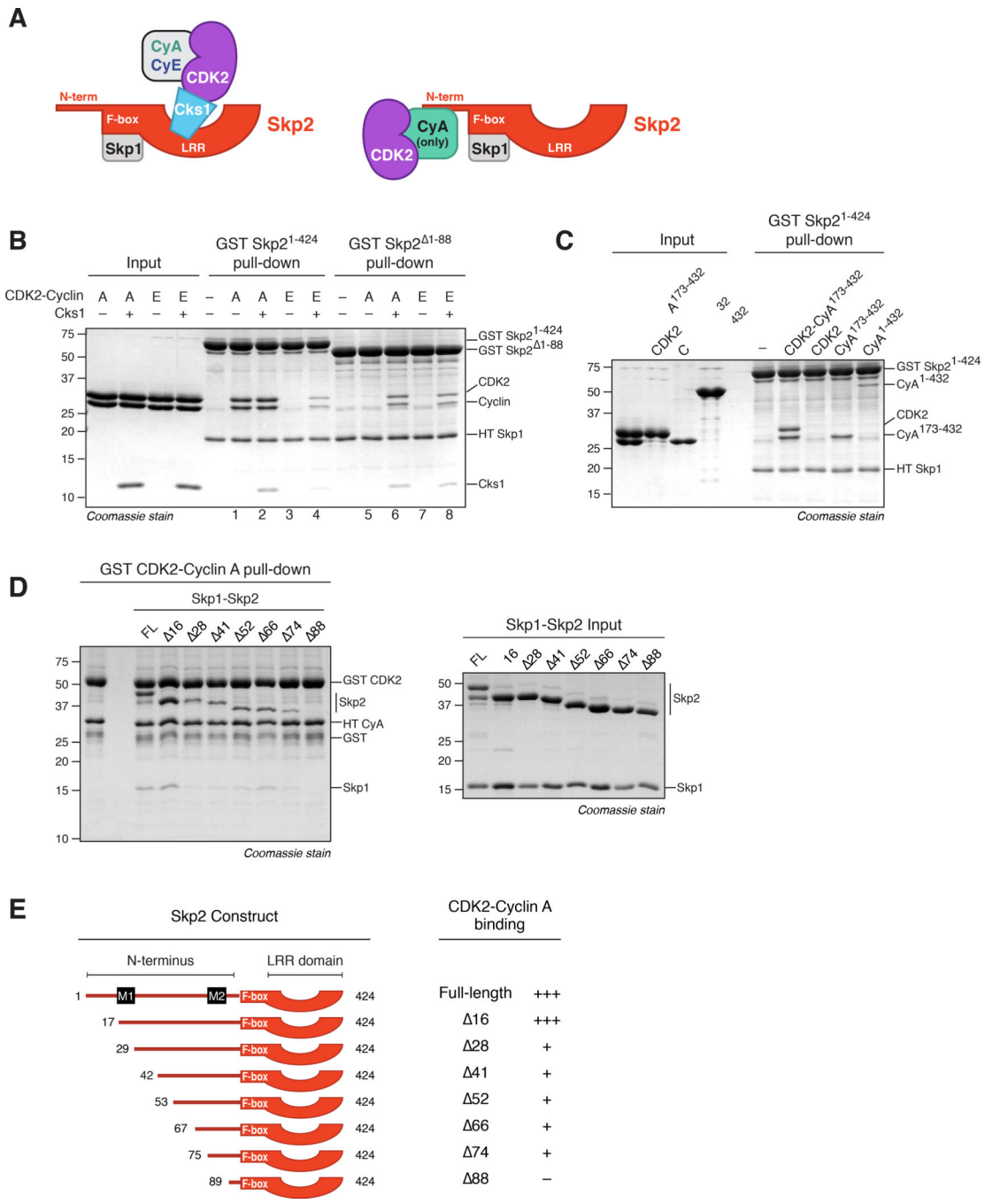

Figure 1. The Skp2 N-terminus contains two motifs that bind cyclin A.

A, Models demonstrating known interactions between Skp1-Skp2 and CDK2-cyclin complexes. Left, the leucine-rich repeat domain (LRR) domain of Skp2 binds both CDK2-cyclin A and CDK2-cyclin E complexes via the bridging adaptor protein Cks1. Right, the N-terminus (N-term) of Skp2 directly binds CDK2-cyclin A complexes without requirement of an adapter protein. Cy denotes cyclin.

B, SDS-PAGE analysis of pull downs using either GST Skp2 full-length (GST Skp2$^{1-424}$) or GST Skp2 lacking the N-terminus (GST Skp2$^{\Delta 1-88}$) to assess binding to CDK2-cyclin

complexes in the presence or absence of the adaptor protein Cks1. Data representative of three separate experiments.

C, SDS-PAGE analysis of pull downs using full-length GST Skp2$^{1-424}$ to assess binding to CDK2 (residues 1–298), cyclin A cyclin domain (CyA$^{173-432}$), full length cyclin A (CyA$^{1-432}$), and CDK2-CyA$^{173–43}$. Data representative of two separate experiments.

D, SDS-PAGE analysis of pull downs using GST CDK2-cyclin A$^{173-432}$ to assess binding to Skp1-Skp2 complexes with indicated deletions in the N-terminus. Data representative of two separate experiments.

E, Summary of pull down results in (D). See Figure S1 for multiple sequence alignment of the N-terminus of Skp2.

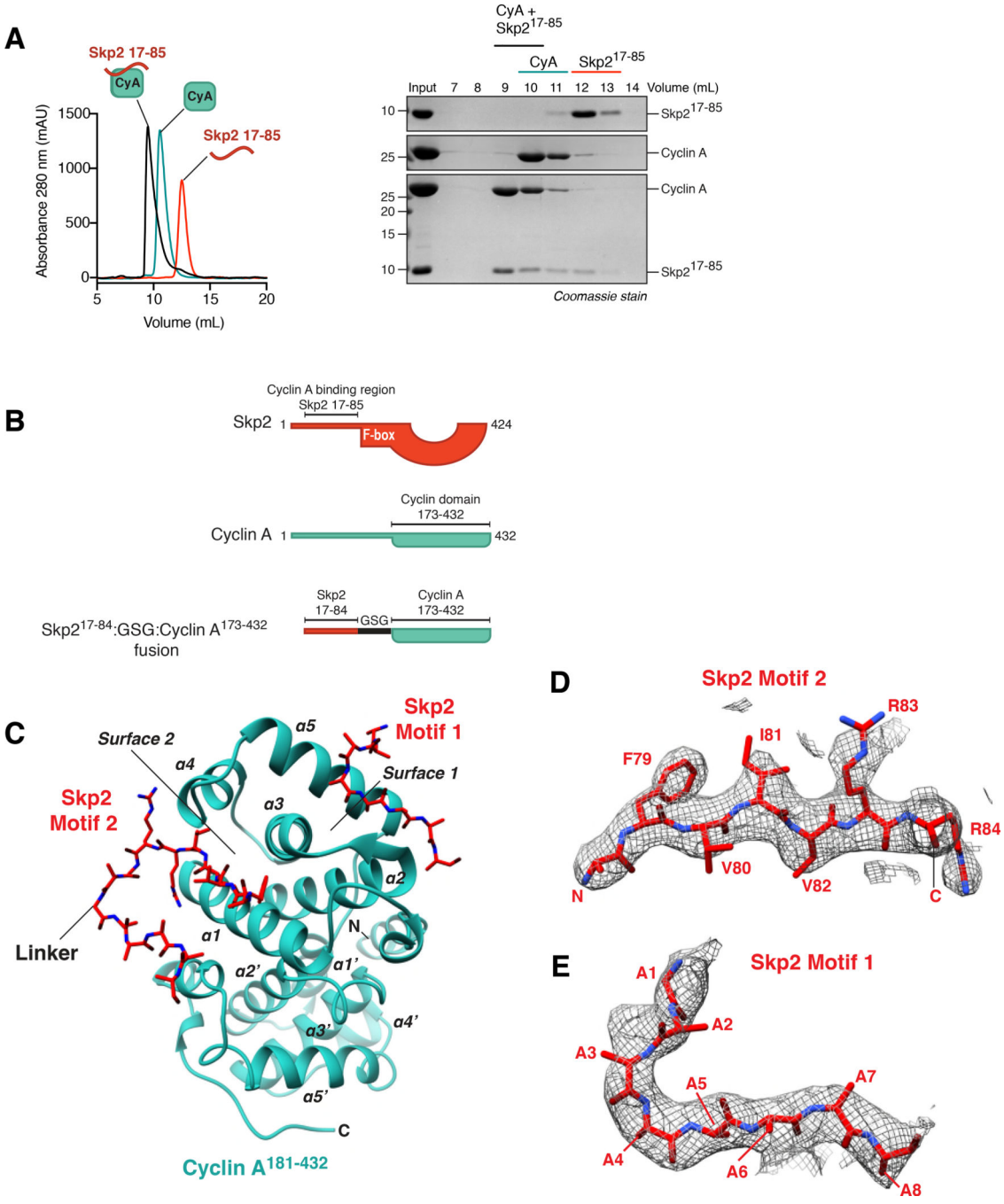

Figure 2. Crystal structure of a fusion between the N-terminus of Skp2 and cyclin A.

A, Size-exclusion profiles (left) of Skp2$^{17-85}$ alone, cyclin A$^{173-432}$ (CyA$^{173-432}$) alone, and Skp2$^{17-85}$ and cyclin A$^{173-432}$ combined with SDS-PAGE analysis (right) of eluted fractions.

B, Schematic of Skp2, cyclin A, and a Skp2:cyclin A fusion construct employed in X-ray crystallography.

C, Crystal structure of Skp2$^{17-84}$:GSG:cyclin A$^{173-432}$. Skp2 is shown in red, cyclin A in blue.

D, Composite omit map contoured to 1σ of 2mFo-DFc density corresponding to Skp2 Motif 2 along cyclin A Surface 2.

E, Composite omit map contoured to 1σ of 2mFo-DFc density corresponding to Skp2 Motif 1 along cyclin A Surface 1.

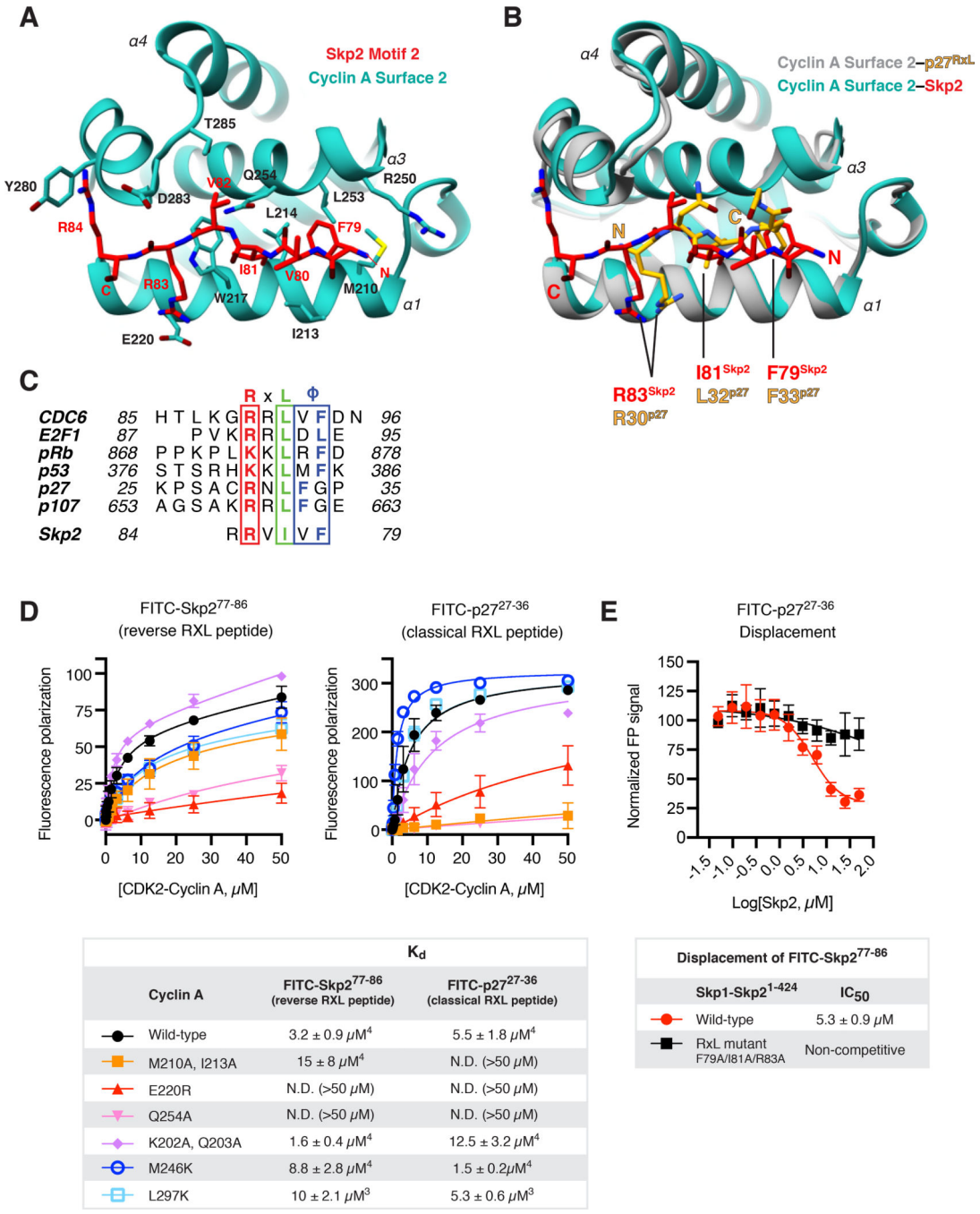

	Cyclin A	K_d FITC-Skp2$^{77-86}$ (reverse RXL peptide)	K_d FITC-p27$^{27-36}$ (classical RXL peptide)
●	Wild-type	3.2 ± 0.9 μM[4]	5.5 ± 1.8 μM[4]
■	M210A, I213A	15 ± 8 μM[4]	N.D. (>50 μM)
▲	E220R	N.D. (>50 μM)	N.D. (>50 μM)
▼	Q254A	N.D. (>50 μM)	N.D. (>50 μM)
◆	K202A, Q203A	1.6 ± 0.4 μM[4]	12.5 ± 3.2 μM[4]
○	M246K	8.8 ± 2.8 μM[4]	1.5 ± 0.2μM[4]
□	L297K	10 ± 2.1 μM[3]	5.3 ± 0.6 μM[3]

	Displacement of FITC-Skp2$^{77-86}$ Skp1-Skp2$^{1-424}$	IC_{50}
●	Wild-type	5.3 ± 0.9 μM
■	RxL mutant F79A/I81A/R83A	Non-competitive

Figure 3. Skp2$^{79-84}$ contains a reverse RxL motif that binds the hydrophobic patch of cyclin A.

A, Zoom in view of cyclin A Surface 2 interacting with Skp2$^{79-84}$ (Motif 2, red).

B, Structure of Skp2$^{17-84}$:GSG:cyclin A$^{173-432}$ fusion superimposed onto the structure of the p27 RxL motif bound to cyclin A (PDB:1H27).

C, Sequence alignment of RxL peptide motifs solved previously bound to the hydrophobic patch of cyclin A.

D, Fluorescence polarization binding analysis of (left) FITC-Skp2$^{77-86}$ (Motif 2, reverse RxL) or (right) FITC-p27$^{27-36}$ (classical RxL) to wild-type or the indicated mutant forms of

CDK2-cyclin A. Quantification summary shown at bottom. Data represents K_d ± SD, N=3 or 4 (denoted as a superscript).

E, Fluorescence polarization analysis comparing the ability of Skp1-Skp2$^{1-424}$ either wild-type or the Motif 2 mutant F79A/I81A/R83A (RxL mutant) to displace FITC-p27$^{27-36}$ from Surface 2 (the hydrophobic patch) of CDK2-cyclin A (6.25 μM). Quantification summary shown at bottom. Data represents IC_{50} ± SD, N=4.

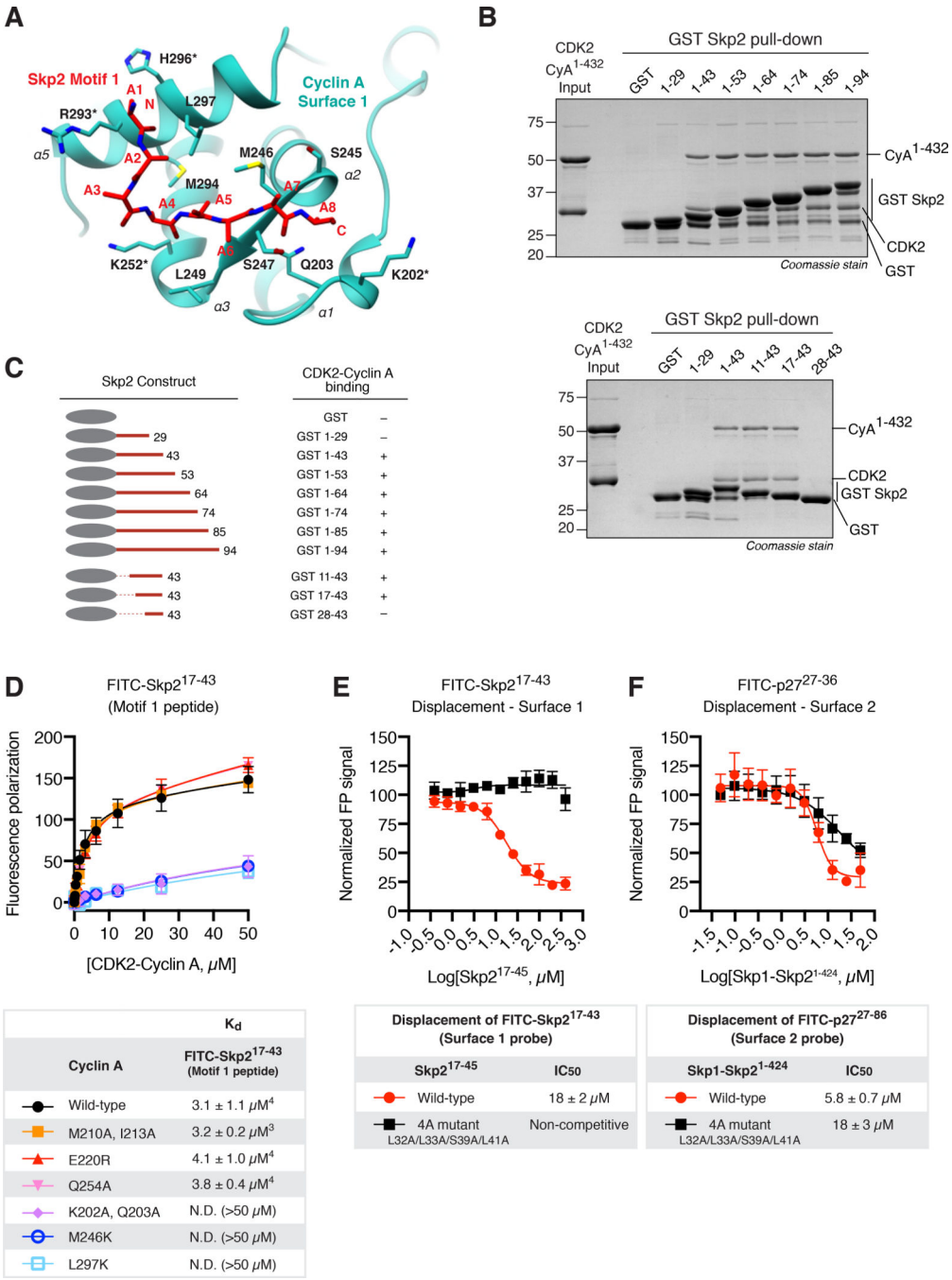

Cyclin A	K_d FITC-Skp2$^{17-43}$ (Motif 1 peptide)
Wild-type	3.1 ± 1.1 μM[4]
M210A, I213A	3.2 ± 0.2 μM[3]
E220R	4.1 ± 1.0 μM[4]
Q254A	3.8 ± 0.4 μM[4]
K202A, Q203A	N.D. (>50 μM)
M246K	N.D. (>50 μM)
L297K	N.D. (>50 μM)

Displacement of FITC-Skp2$^{17-43}$ (Surface 1 probe)	
Skp2$^{17-45}$	IC50
Wild-type	18 ± 2 μM
4A mutant L32A/L33A/S39A/L41A	Non-competitive

Displacement of FITC-p27$^{27-86}$ (Surface 2 probe)	
Skp1-Skp2$^{1-424}$	IC50
Wild-type	5.8 ± 0.7 μM
4A mutant L32A/L33A/S39A/L41A	18 ± 3 μM

Figure 4. An undetermined eight residue element denoted Motif 1 within Skp2$^{17-43}$ binds Surface 1 of cyclin A.

A, Polyalanine chain representing an eight residue motif in Skp2 (Motif 1) bound to cyclin A Surface 1 (directionality N' to C' undetermined). Side chains of residues marked with an asterisk were modelled for clarity.

B, SDS-PAGE analysis of pull-downs using the indicated GST-tagged fragments of the Skp2 N-terminus to assess binding to CDK2-cyclin A$^{1-432}$ (CyA$^{1-432}$). Data representative of two separate experiments.

C, Summary of GST pull-down results in (B). See Figure S1 for multiple sequence alignment of the N-terminus of Skp2.

D, Fluorescence polarization binding analysis of FITC-Skp2$^{17-43}$ (Motif 1) to wild-type or the indicated mutant forms of CDK2-cyclin A. Quantification summary shown at bottom. Data represents K_d ± SD, N=3 or 4 (denoted as a superscript).

E, Fluorescence polarization analysis comparing the ability of Skp2$^{17-45}$ either wild type or the Motif 1 mutant L32A/L33A/S39A/L41A (4A mutant) to displace FITC-Skp2$^{17-43}$ peptide from CDK2-cyclin A (15 μM). Quantification summary shown at bottom. Data represents IC_{50} ± SD, N=4.

F, Fluorescence polarization analysis comparing the ability of Skp1-Skp2$^{1-424}$ either wild type or the Motif 1 mutant L32A/L33A/S39A/L41A (4A mutant) to displace FITC-p27$^{27-36}$ peptide from CDK2-cyclin A (6.25 μM). Quantification summary shown at bottom. Data represents IC_{50} ± SD, N=4.

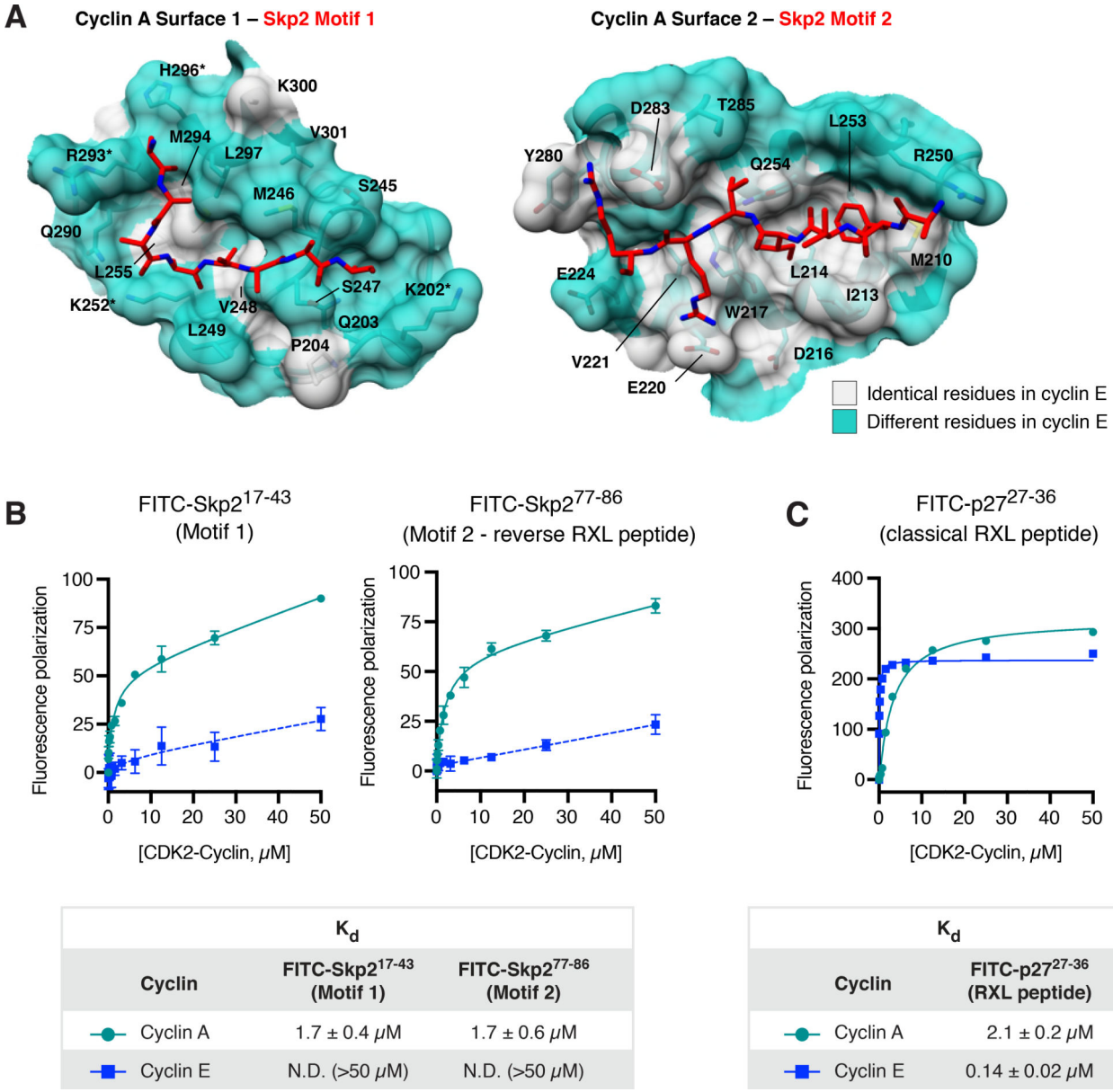

	K_d	
Cyclin	FITC-Skp2$^{17-43}$ (Motif 1)	FITC-Skp2$^{77-86}$ (Motif 2)
Cyclin A	1.7 ± 0.4 μM	1.7 ± 0.6 μM
Cyclin E	N.D. (>50 μM)	N.D. (>50 μM)

	K_d
Cyclin	FITC-p27$^{27-36}$ (RXL peptide)
Cyclin A	2.1 ± 0.2 μM
Cyclin E	0.14 ± 0.02 μM

Figure 5. Both Skp2 Motifs 1 and 2 bind to CDK2-cyclin A and not CDK2-cyclin E.

A, Zoom in view of (left) cyclin A Surface 1 indicating residues conserved (grey) or non-conserved (teal) with cyclin E, and (right) cyclin A Surface 2 (hydrophobic patch) indicating residues conserved (grey) and non-conserved (teal) with cyclin E. Side chains of residues marked with an asterisk were modelled for clarity.

B, Fluorescence polarization binding analysis of (left) FITC-Skp2$^{17-43}$ or (right) FITC-Skp2$^{77-86}$ binding to CDK2-cyclin A$^{173-432}$ or CDK2-cyclin E$^{96-378}$. Quantification summary shown at bottom. Data represents K_d ± SD, N=4.

C, Fluorescence polarization binding analysis of FITC-p27$^{27-36}$ (classical RxL) binding to CDK2-cyclin A$^{173-432}$ or CDK2-cyclin E$^{96-378}$. Quantification summary shown at right. Data represents Kd ± SD, N=4.

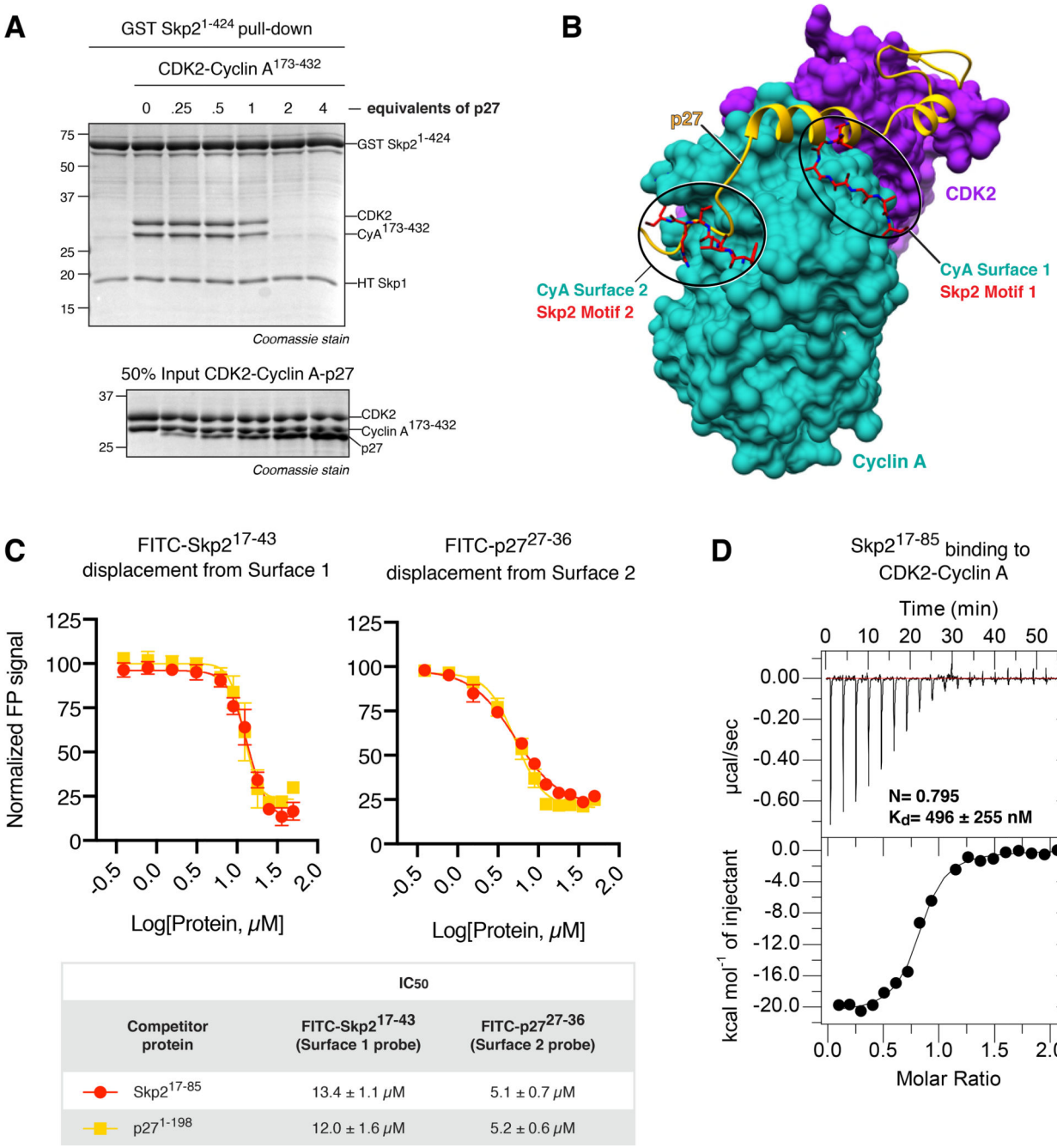

	IC50	
Competitor protein	FITC-Skp2^17-43 (Surface 1 probe)	FITC-p27^27-36 (Surface 2 probe)
Skp2^17-85	13.4 ± 1.1 μM	5.1 ± 0.7 μM
p27^1-198	12.0 ± 1.6 μM	5.2 ± 0.6 μM

Figure 6. Both p27 and the N-terminus of Skp2 bind Surface 1 and Surface 2 of cyclin A.

A, SDS-PAGE analysis of pull-downs using GST Skp2$^{1-424}$ (5 μM) to assess binding to CDK2-cyclin A (5 μM) in absence or presence of increasing concentrations of p27$^{1-198}$ (0–20 μM). Data representative of two separate experiments.

B, Superposition of Skp2 Motif 1 and Motif 2 onto the crystal structure of p27$^{25-93}$ bound to CDK2-cyclin A (PDB:1JSU).

C, Fluorescence polarization analysis comparing the ability of Skp2$^{17-85}$ and p27$^{1-198}$ to displace (left) FITC-Skp2$^{17-43}$ from CDK2-cyclin A (15 μM) or (right) FITC-p27$^{27-36}$ from

CDK2-cyclin A (6.25 μM). Quantification summary shown at bottom. Data represents IC_{50} ± SD, N=4.

D, ITC (isothermal calorimetry) analysis of binding between $Skp2^{17-85}$ and CDK2-cyclin A. Data represents K_d ± SD, N=3. Only one representative ITC trace is shown.

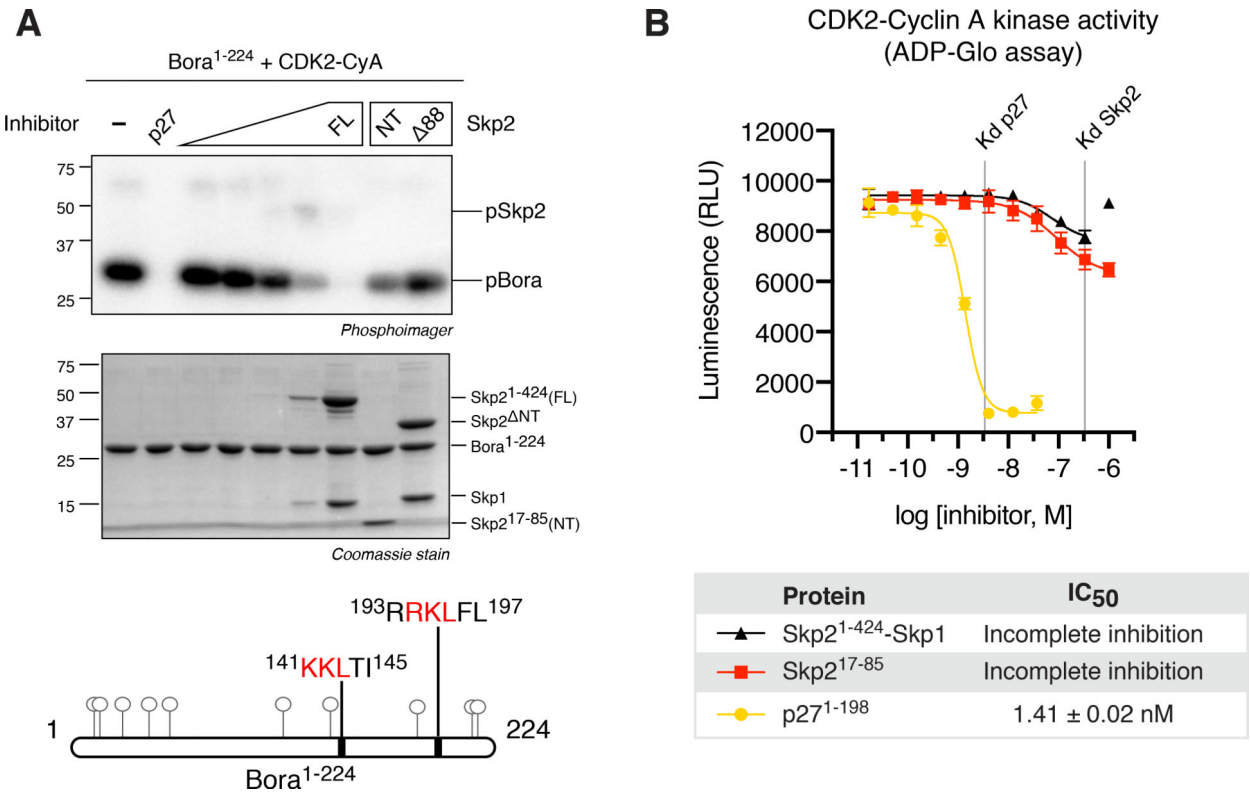

Protein	IC_{50}
$Skp2^{1-424}$-Skp1	Incomplete inhibition
$Skp2^{17-85}$	Incomplete inhibition
$p27^{1-198}$	1.41 ± 0.02 nM

Figure 7. The N-terminus of Skp2 is an inhibitor of CDK2-cyclin A.

A, Phosphoimager (top) and SDS-PAGE (middle) analysis of $Bora^{1-224}$ phosphorylation by CDK2-cyclin A (3 nM) in the presence of $p27^{1-198}$ (10 nM), increasing concentrations of Skp1-$Skp2^{1-424}$ (1 nM – 10,000 nM), $Skp2^{17-85}$ or Skp1-$Skp2^{\Delta 1-88}$ (10,000 nM). Schematic of $Bora^{1-224}$ fragment highlighting RxL targeting motifs and Ser/Thr phospho-acceptor sites shown at bottom. Data representative of three separate experiments.

B, ATPase activity analysis of CDK2-cyclin A in the presence of increasing concentrations of $p27^{1-198}$, $Skp2^{17-85}$, or Skp1-$Skp2^{1-424}$. Data represents IC_{50} ± SD, N=3.

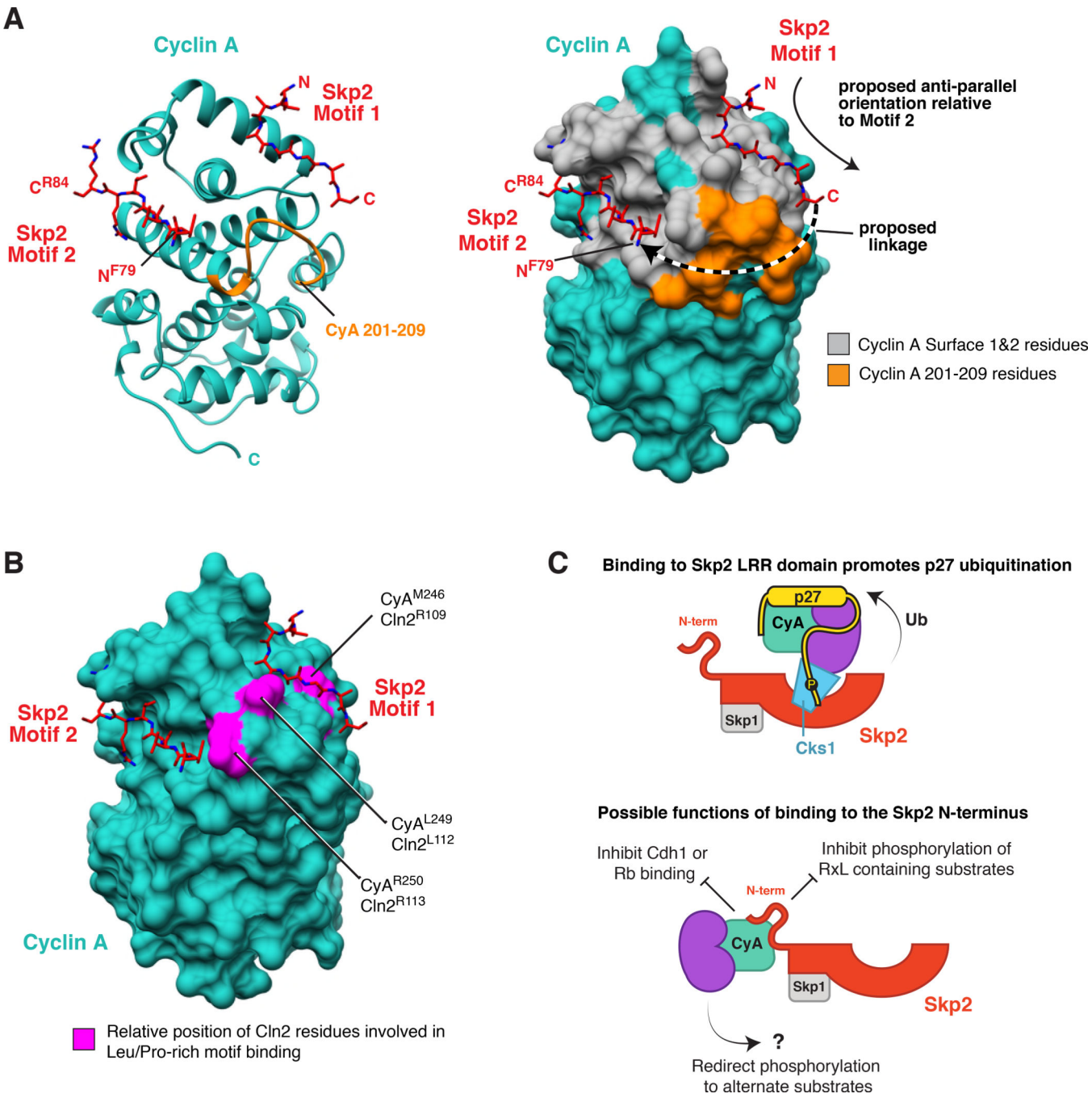

Figure 8. Hypothetical connectivity of Skp2 Motifs 1 and 2 bound to cyclin A.

A, Ribbon (left) and surface (right) representation of Skp2 binding to cyclin A. Highlighted in orange is the position of a loop region in cyclin A comprised of residues 201 to 209 implicated in binding Skp2 via HDX-MS experiments (Salamina et al., 2021). An antiparallel arrangement of Skp1 Motif 2 relative to Skp2 Motif 1 allows connectivity in a manner that overlaps with cyclin A residues 201 to 209.

B, Surface representation of human cyclin A indicating the relative position of residues in *S. cerevisiae* cyclin Cln2 implicated in binding short linear motifs enriched in Leu and Pro.

C, Models demonstrating the known and possible biological functions of Skp2 binding to CDK2-cyclin A complexes. Top, the LRR domain of Skp2 binds to p27-CDK2-cyclin A complexes via the bridging adaptor protein Cks1 to mediate p27 ubiquitination by SCFSkp2. Bottom, possible functions for the N-terminus of Skp2 binding to CDK2-cyclin A.

Table 1.

Diffraction data collection and refinement statistics.

	Skp2$^{17–84}$:GSG:cyclin A$^{173–432}$
Data collection	
Space group	P 4 2_1 2
Cell dimensions	
a, *b*, *c* (Å)	109.74, 109.74, 152.03
$\alpha\beta\gamma$ (°)	90.00, 90.00, 90.00
Resolution (Å)	109.74–3.17 (3.39–3.17)
R_{meas}	0.217 (1.7373)
R_{pim}	0.073 (0.581)
$I/\sigma I$	10.3 (1.4)
$CC_{1/2}$	0.996 (0.439)
Completeness (%)	99.8 (100.0)
Reflections (unique)	16322 (2909)
Redundancy	8.8 (9.1)
Refinement	
Resolution (Å)	88.98–3.17 (3.23–3.17)
No. reflections	16268 (1574)
R_{work}	0.231 (0.3514)
R_{free}	0.277 (0.3927)
No. atoms	
Protein	4106
B-factors	
Protein (overall)	80.43
Cyclin A	79.46
Skp2 Motif 1	109.15
Skp2 Motif 2 + Linker	89.94
R.M.S. deviations	
Bond lengths (Å)	0.001
Bond angles (°)	0.370
Ramachandran Plot	
Most favored (%)	99.26
Allowed (%)	0.74
Disallowed (%)	0.00
Clashscore	2.51
MolProbity score	1.03
PDB ID code	7LUO

*Highest resolution shell is shown in parenthesis.

KEY RESOURCES TABLE

REAGENT or RESOURCE	SOURCE	IDENTIFIER
Bacterial and virus strains		
BL21(DE3) chemically competent *E.coli*	ThermoFisher	Cat# C600003
DH5alpha chemically competent *E. coli*	ThermoFisher	Cat# EC0112
Chemicals, peptides, and recombinant proteins		
FITC-Skp2$^{17–43}$ peptide	This paper	N/A
FITC-Skp2$^{77–86}$ peptide	This paper	N/A
FITC-p27$^{27–36}$ peptide	This paper	N/A
Bora$^{1–224}$	Gift from Nicolas Tavernier (Institut Jacques Monod)	N/A
Critical commercial assays		
ADP-Glo™ assay	Promega Corporation	Cat# V6930
Deposited data		
Crystal structure of Skp2$^{17–84}$:GSG:cyclin A$^{173–432}$	This paper	PDB: 7LUO
Crystal structure of CDK2-cyclin A	Jeffrey et al., 1995	PDB:1FIN
Crystal structure of CDK2-cyclin A-p27$^{25–35}$	Lowe et al., 2002	PDB:1H27
Crystal structure of CDK2-cyclin A-p27$^{23–106}$	Russo et al., 1996	PDB:1JSU
Experimental models: organisms/strains		
Oligonucleotides		
Additional oligonucleotides listed in Supplementary Table 1		
NcoI Skp2 N17: TCGACCATGGGAGCCACCAGCTTCACGTGG	Millipore Sigma	N/A
Skp2(84):GSG:cyclin A(173) primer F: GTCTGGTACTTCATTTCCTGATCCCCTGCGGACAATCACAAAGTC	Millipore Sigma	N/A
Skp2(84):GSG:cyclin A(173) primer R: GATTGTCCGCAGGGGATCAGGAAATGAAGTACCAGACTACCATGAGG	Millipore Sigma	N/A
SacI Cyclin A C432: TCAGGAGCTCTCACAGATTTAGTGTCTCTGGTGGGTTGAG	Millipore Sigma	N/A
Recombinant DNA		
pGEX 4T-3 CDK2 (human 1–298)	Gift from Tanja Mittag (St. Jude Children's Research Hospital)	BC003065
pProEX Cyclin A (human 1–432)	This paper	BC104783
pProEX Cyclin A (human 173–432)	This paper	BC104783
pProEX Cyclin E (human 96–378)	This paper	BC035498
pProEX p27 (human 1–198)	This paper	BC001971
pGEX Cks1 (human 1–79)	This paper	BC015629
pGEX Skp1 (crystal construct) – Skp2 (human 1–424)	This paper	BC065730, BC007441

REAGENT or RESOURCE	SOURCE	IDENTIFIER
pGEX Skp1 (crystal construct) – Skp2 (human 17–424)	This paper	BC065730, BC007441
pGEX Skp1 (crystal construct) – Skp2 (human 29–424)	This paper	BC065730, BC007441
pGEX Skp1 (crystal construct) – Skp2 (human 42–424)	This paper	BC065730, BC007441
pGEX Skp1 (crystal construct) – Skp2 (human 53–424)	This paper	BC065730, BC007441
pGEX Skp1 (crystal construct) – Skp2 (human 67–424)	This paper	BC065730, BC007441
pGEX Skp1 (crystal construct) – Skp2 (human 75–424)	This paper	BC065730, BC007441
pGEX Skp1 (crystal construct) – Skp2 (human 89–424)	This paper	BC065730, BC007441
pGEX Skp2 - human 1–94	This paper	BC007441
pGEX Skp2 - human 1–85	This paper	BC007441
pGEX Skp2 - human 1–74	This paper	BC007441
pGEX Skp2 - human 1–64	This paper	BC007441
pGEX Skp2 - human 1–53	This paper	BC007441
pGEX Skp2 - human 1–43	This paper	BC007441
pGEX Skp2 - human 1–29	This paper	BC007441
pGEX Skp2 - human 11–43	This paper	BC007441
pGEX Skp2 - human 17–43	This paper	BC007441
pGEX Skp2 - human 17–45	This paper	BC007441
pGEX Skp2 - human 28–43	This paper	BC007441
pGEX Skp2$^{17–84}$:GSG:cyclin A$^{173–432}$	This paper	BC007441, BC104783
Software and algorithms		
Adobe Photoshop (version 22.2.0)	Adobe	www.adobe.com
XDS (version 20170601)	Kabsch, 2010	https://xds.mr.mpg.de
Phaser (version 2.8.3)	McCoy et al., 2007	https://www-structmed.cimr.cam.ac.uk/phaser_obsolete/
PHENIX (version 1.17)	Adams et al., 2011	https://www.phenix-online.org/download/
Coot (version 0.9)	Emsley et al., 2010	https://www2.mrc-lmb.cam.ac.uk/personal/pemsley/coot/
Chimera (version 1.14)	Pettersen et al., 2004	www.cgl.ucsf.edu/chimera/
Clustal Omega	Sievers et al., 2011	www.ebi.ac.uk/Tools/msa/clustalo/
Jalview (version 2.11.1.4)	Waterhouse et al., 2009	https://www.jalview.org
Excel (version 16.16.27)	Microsoft	www.microsoft.com
GraphPad Prism (version 8.2.1)	GraphPad	www.graphpad.com
Origin 7 (version 7.0552)	Malvern Panalytical	www.malvernpanalytical.com